Improving Subsurface Stress Characterization for Carbon Dioxide Storage Projects by Incorporating Machine Learning Techniques

(DE-FE0031684)

Dr. William Ampomah – New Mexico Tech – PRRC

Dr. Lianjie Huang – Los Alamos National Laboratory

Donald Lee - Consultant

U.S. Department of Energy

National Energy Technology Laboratory
Carbon Management Project Review Meeting
August 15 - 19, 2022

Outline

- Project overview
- Project objectives
- Technical Approach
- Accomplishments
- Summary

Project Overview

– Funding Profile

– Project Performance Dates:

10/01/2018 – 09/30/2022

	Budget		Expenditure						Remaining Balance	
	Project Year 1 through 3		Oct 2021 - Dec 2021 (Y4 Q1)		Jan 2022 - Mar 2022 (Y4 Q2)		Apr 2022 - Jun 2022 (Y4 Q3)		Project Year 4	
	DOE	Cost share	DOE	Cost share	DOE	Cost share	DOE	Cost share	DOE	Cost share
New Mexico Tech (Recipient) - Cash	$ 952,264.00	$ 193,090.66	$25,181.52	$ 2,252.79	$12,326.42	$ 3,093.76	$17,246.39	$ 9,059.77	$ 52,993.93	$ 17,070.67
Schlumberger Technology - InKind	$ -	$ 234,070.00	$ -	$8,517.50	$ -	$8,517.50	$ -	$8,517.50	$ -	$ 8,517.49
Non-FFRDC Subtotal:	$ 952,264.00	$ 427,160.66	$ 25,181.52	$ 10,770.29	$ 12,326.42	$ 11,611.26	$ 17,246.39	$ 17,577.27	$ 52,993.93	$ 25,588.16
Sandia National Lab	$ 100,000.00	$ -	$ -	$ -	$ -	$ -	$ -	$ -	$ -	$ -
Los Alamos National Lab	$ 610,000.00	$ -	$23,097.99	$ -	$ 52,115.14	$ -	$ 49,634.99	$ -	$ 57,914.33	$ -
FFRDC Subtotal:	$ 710,000.00	$ -	$ 23,097.99	$ -	$ 52,115.14	$ -	$ 49,634.99	$ -	$ 57,914.33	$ -
Grant Total	$ 1,662,264.00	$ 427,160.66	$ 48,279.51	$ 10,770.29	$ 64,441.56	$ 11,611.26	$ 66,881.38	$ 17,577.27	$ 110,908.26	$ 25,588.16

Acknowledgments

We thank DOE/NETL for the award opportunity through DE-FE0031684 and our partners.

Project Team

New Mexico Tech

Dr. William Ampomah (PI)
Dr. Robert Balch
Mr. George El-Kasseh
Ms. Martha Cather

LANL

Dr. Lianjie Huang (Co-PI)
Dr. Xuejian Liu (postdoc)
Dr. Yan Qin (postdoc)
Dr. Jiaxuan Li (GRA)
Dr. Kai Gao

Consultants

Dr. Tom Bratton
Mr. Donald Lee

Students

Ms. Marcia McMillan

Program Overview

Goals and Objectives

- The primary objective is to develop a framework to boost the reliability of characterization and prediction of the state of stress in the overburden and underburden in CO_2 storage reservoirs using novel machine learning and integrated geomechanics and geophysical methods.

- We use field data and models developed by the Southwest Regional Partnership on Carbon Sequestration (SWP) for the Farnsworth Unit (FWU), a CO_2 enhanced oil recovery (EOR) project Ochiltree County, Texas, to verify the improved capabilities of our methods.

Technology/Site Selection

- Demonstrated at the Farnsworth Unit ongoing CO_2 EOR development:
  - Discovered 1956
  - Primary depletion until~ 1965
  - Waterflood until ~2010
  - CO2 WAG EOR Started 2010
- Extensive characterization dataset previously was acquired, and modeling performed by the SWP partnership

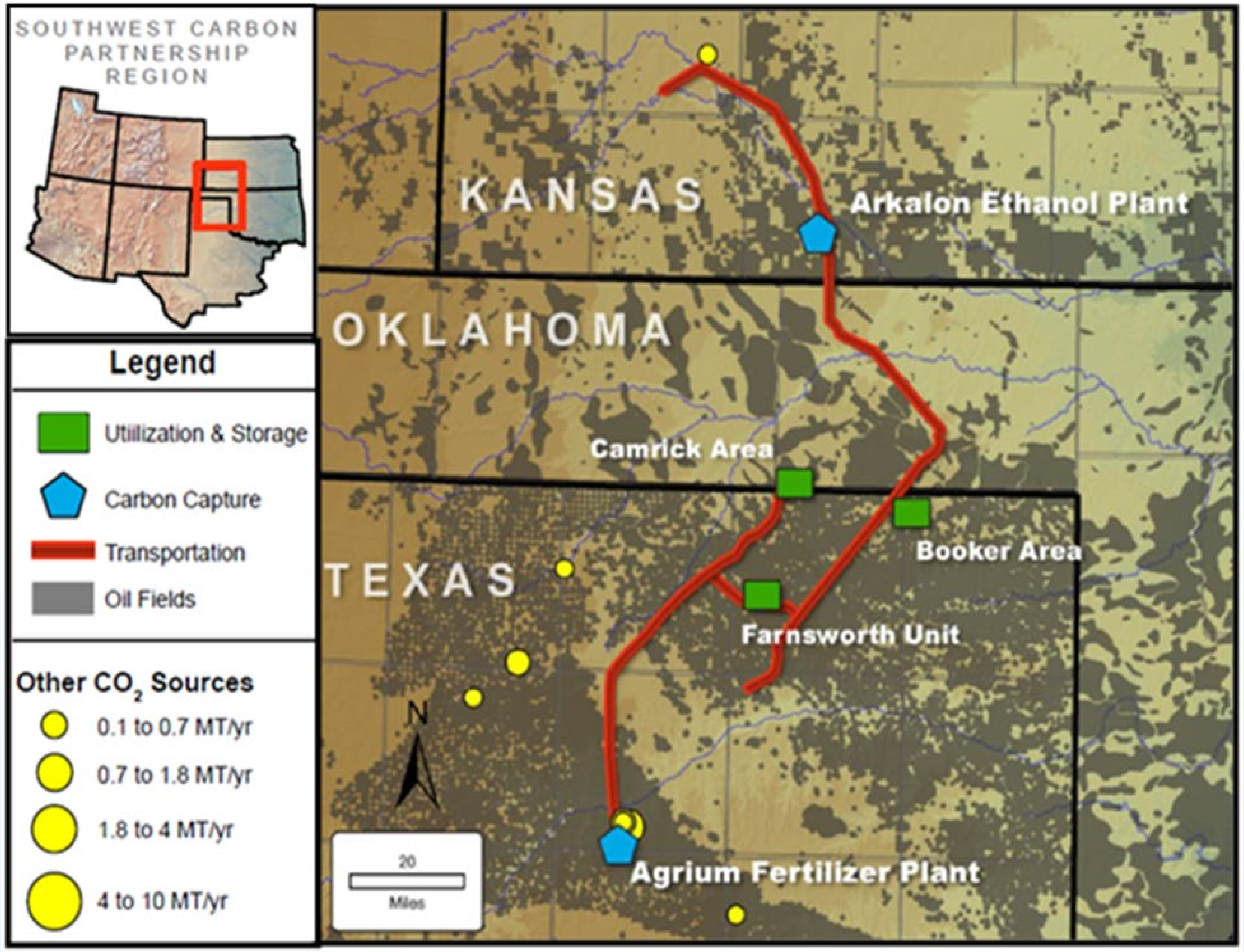

Technical Approach/Project Scope

- The final outcome of this work will be a methodology for integration of multi-disciplinary data to reduce uncertainty in estimation of stress changes in the storage complex and underburden.
- Significant project risks include stress-sensitivity of rock behavior under anticipated effective stress changes, and microseismic data characteristics.
- The robust characterization dataset which includes extensive geological, geophysical, and geomechanical, and seismological data provide opportunities for technical risk mitigation through alternative integration strategies.

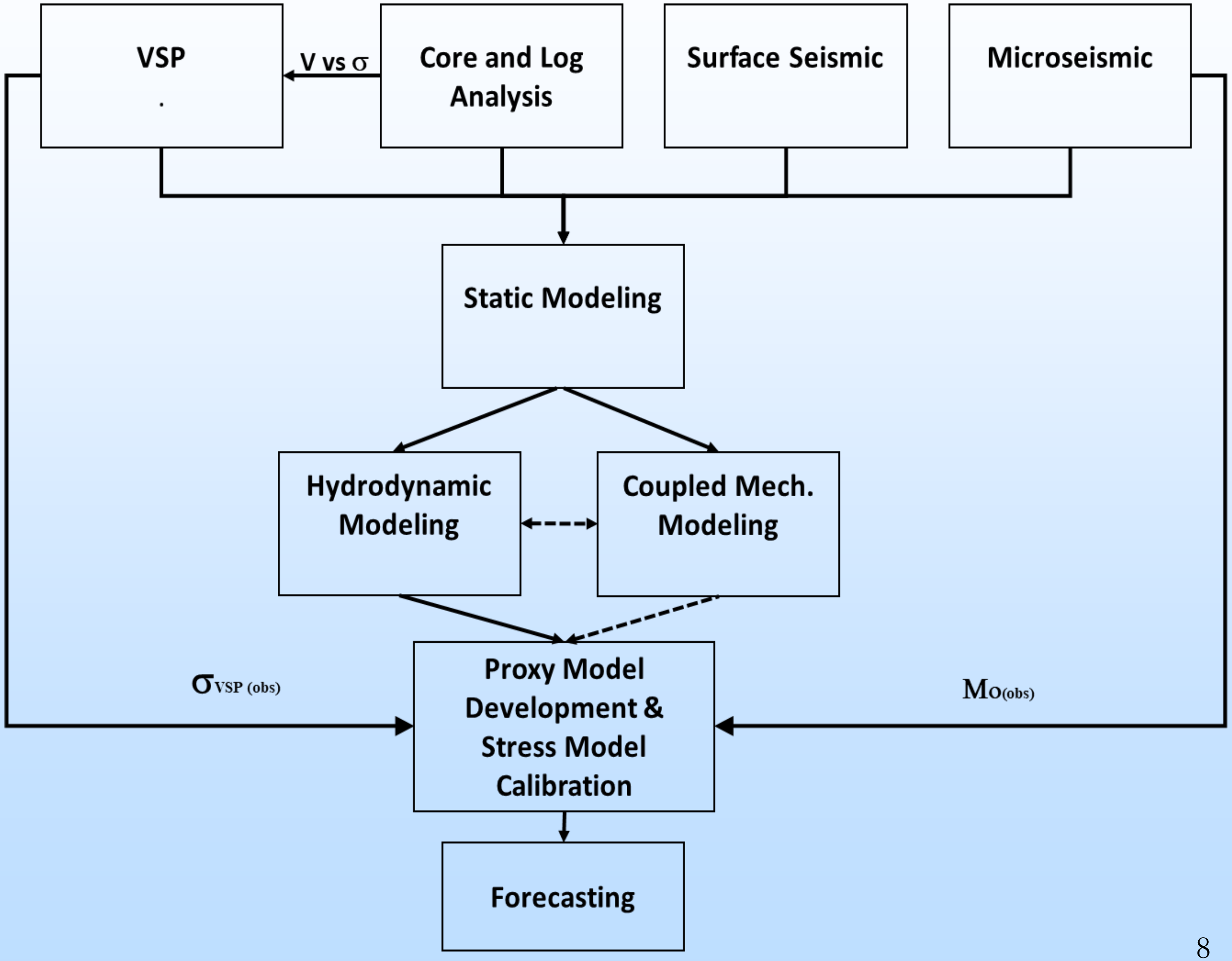

Technical Approach/Project Scope

Task/ Subtask	Milestone Title	Planned Completion	Status
1	Project Management Plan	1/31/2018	PMP file
1	Kickoff Meeting	11/31/18	Completed
2.2	1D MEM Model	2/28/2019	Completed
2.4	VSP Elastic Inversion	10/31/2019	Completed
2.6	VSP Stress Estimation	2/28/2019	Completed
3	Microseismic Analysis	8/31/2022	Ongoing
4	3D MEM Model	9/30/2019	Completed
5	Hydrodynamic History Matching	3/31/2020	Completed
6	Evaluation of one-way and two-way coupling process	8/30/2020	Completed
7.1	Stress Objective function formulation	7/30/2020	Completed
7.4/7.5	Completion of VSP - history matching	5/31/2021	Completed
7.4/7.5	Microseismic- Geomechanics history match	9/30/2022	Ongoing
8	Forecasting pressure and stress	8/30/2021	Completed

VSP Integration Workflow

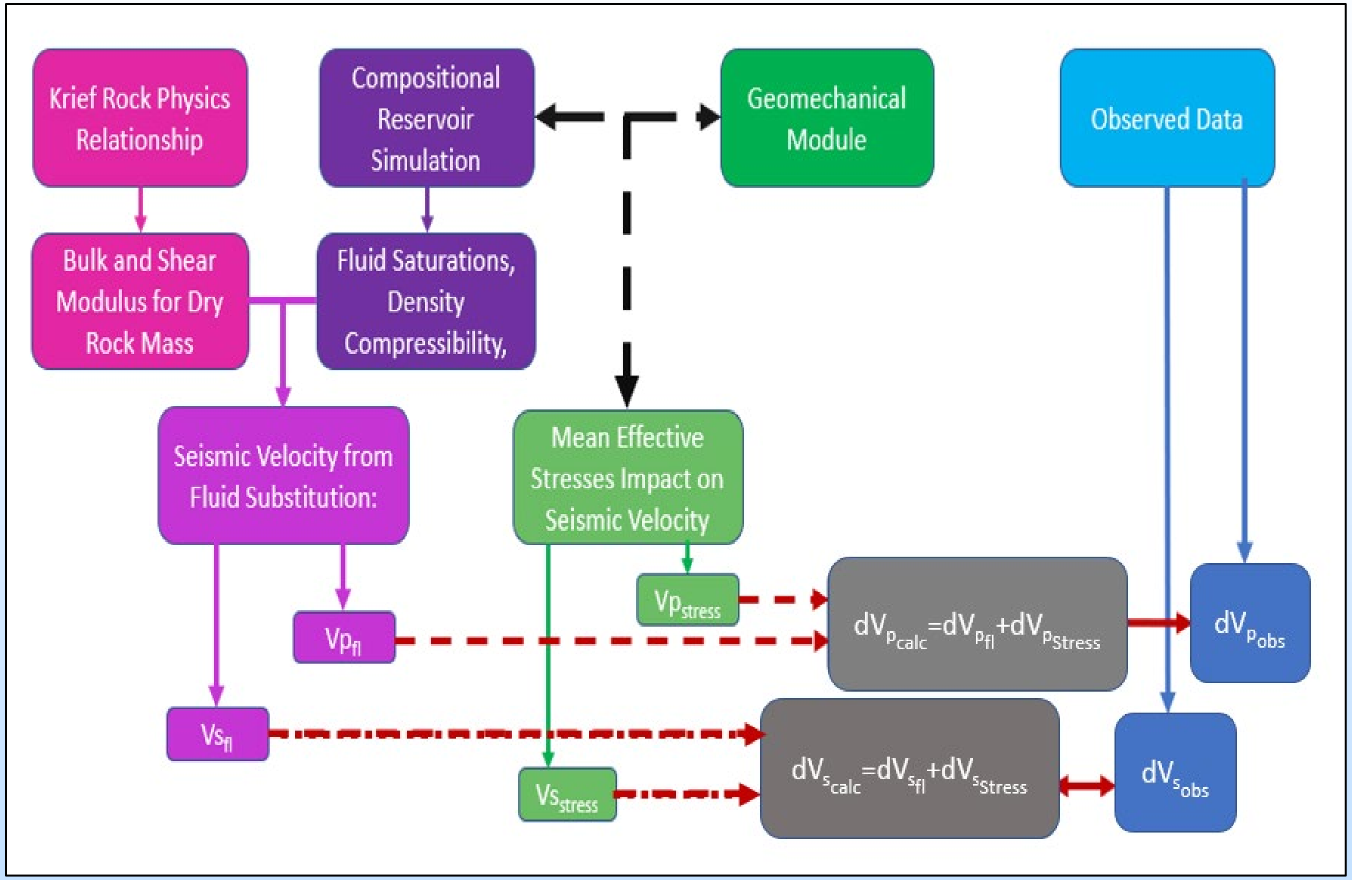

Modelled Seismic Velocity:

Based on the Principle of Superposition

$$dV^{mon}{}_{modeled} = dV^{mon}{}_{fluid} + dV^{mon}{}_{stress} \; ,$$

dV= dVp , dVs

Seismic Velocity Mismatch:

$$dV^{mon}{}_{mismatch} = dV^{mon}{}_{modelled} - dV^{mon}{}_{obs} \; ,$$

dV= dVp , dVs

VSP Objective Function Formulation: *Task 7.3*

Summation of all six(6) seismic velocity mismatches

$$VSP\ Objective = \sum dV^{mon}$$

dV= dVp , dVs ***mon= 1,2,3***

Goal: Minimization of the VSP Objective Function

Geological and Geomechanical Static Modeling

- The geological model developed by SWP has been updated with structural and stratigraphic reinterpretation of newly depth imaged seismic data.
- The updated model extends from ground surface to below the injection zone (Morrow B reservoir).
- Petrophysical properties of the reservoir and caprock have been updated through integration of geophysical logs, core, and seismic elastic inversion products.
- Elastic properties of the reservoir, underburden, and overburden have been updated through integration of well data based 1-D Mechanical Earth Models (MEM) derived from geophysical logs and core analysis.

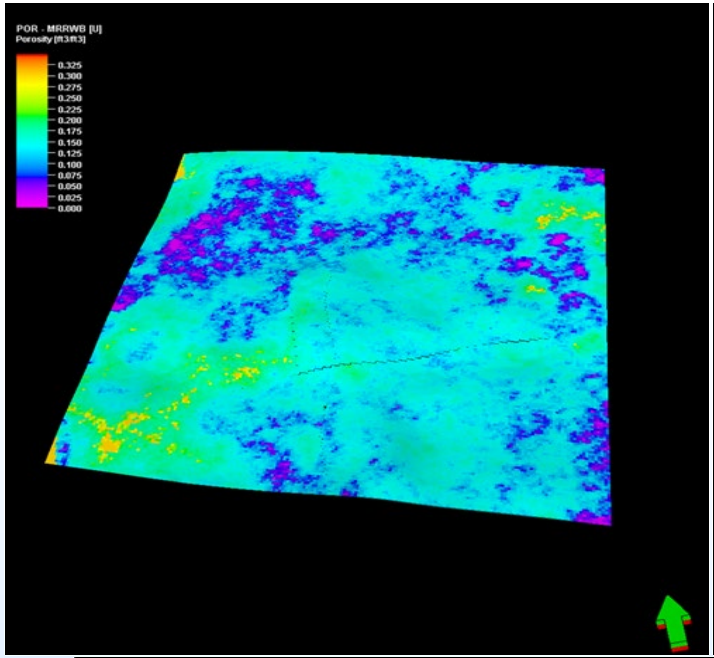

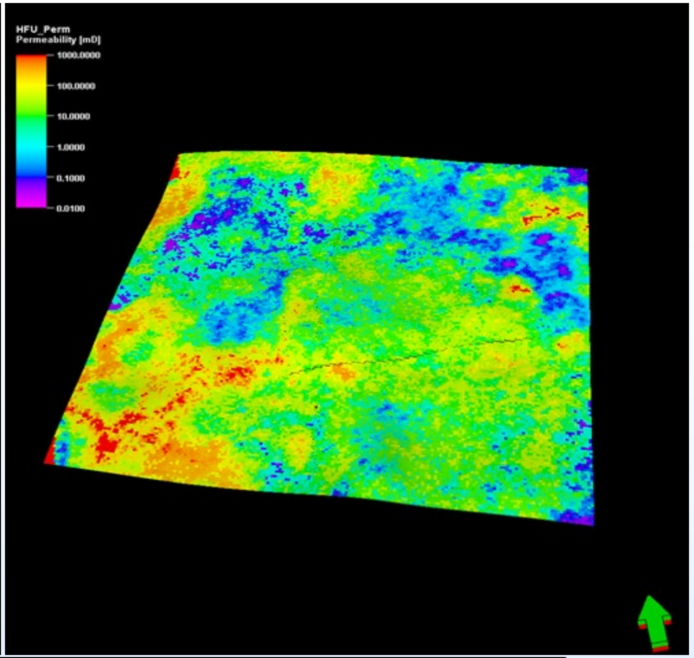

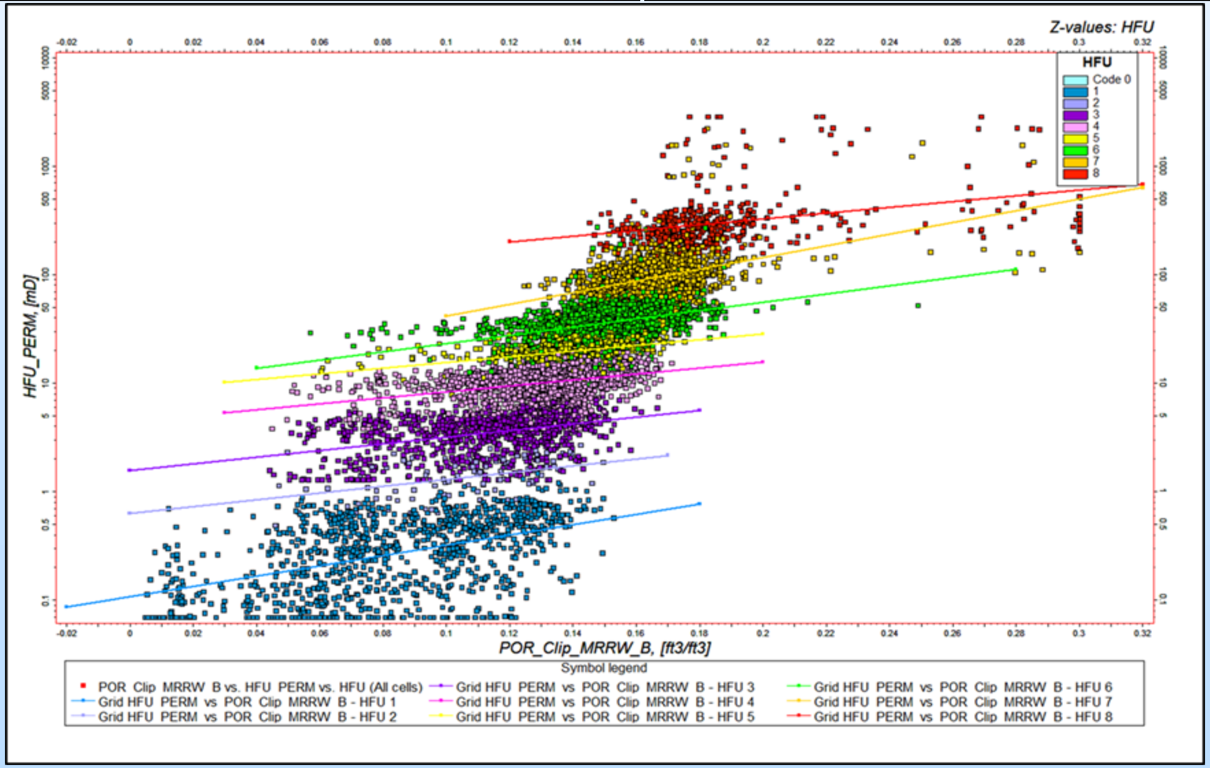

Hydrodynamic Flow Calibration

- Primary/Secondary (pressure depletion/waterflood) and tertiary (CO2 WAG) periods were history matched using proxy modeling and machine learning optimization.
- Separate proxy models were developed for primary/secondary and CO2 WAG development periods each using 100 full physics runs to train and verify proxy models.
- Particle swarm optimization was employed and coupled with the proxy models to minimize the history matching error
- Optimized reservoir parameters were verified in full physics simulations.

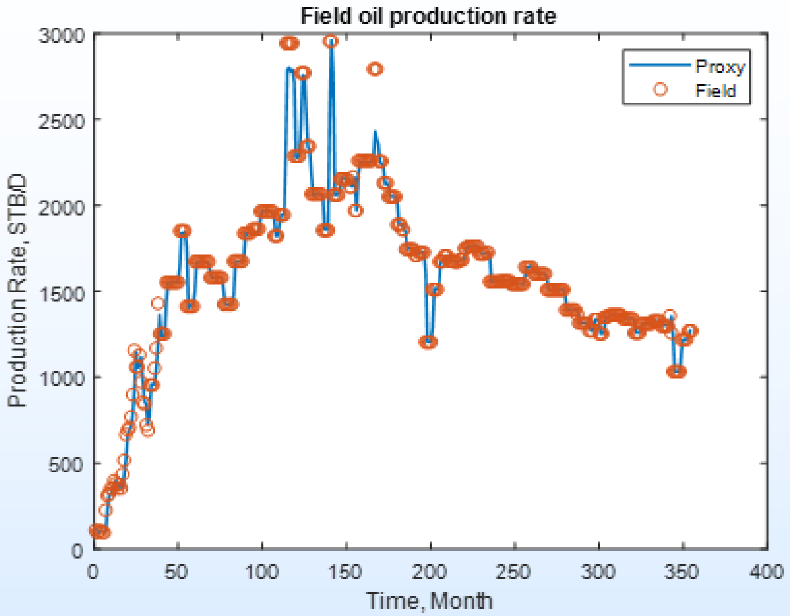

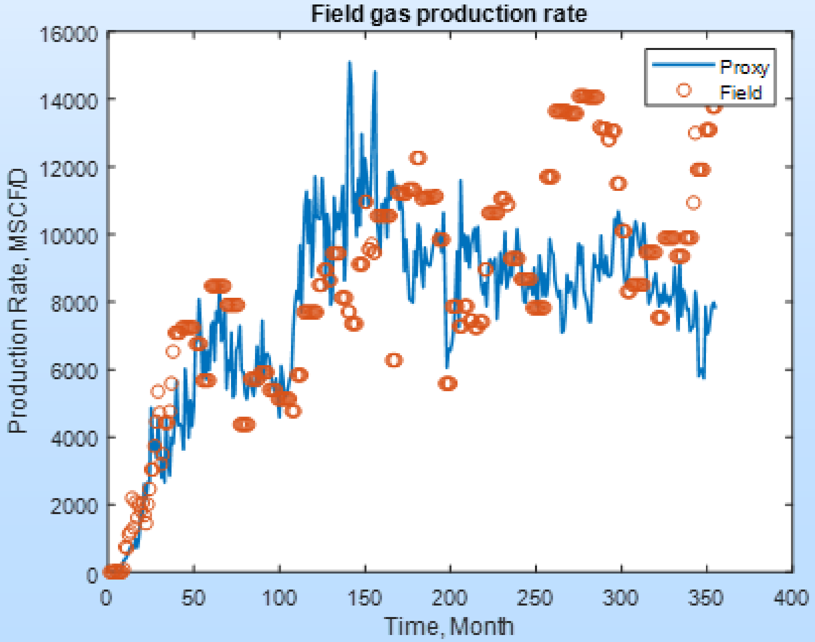

VSP- Geomechanical Calibration Task 7.4

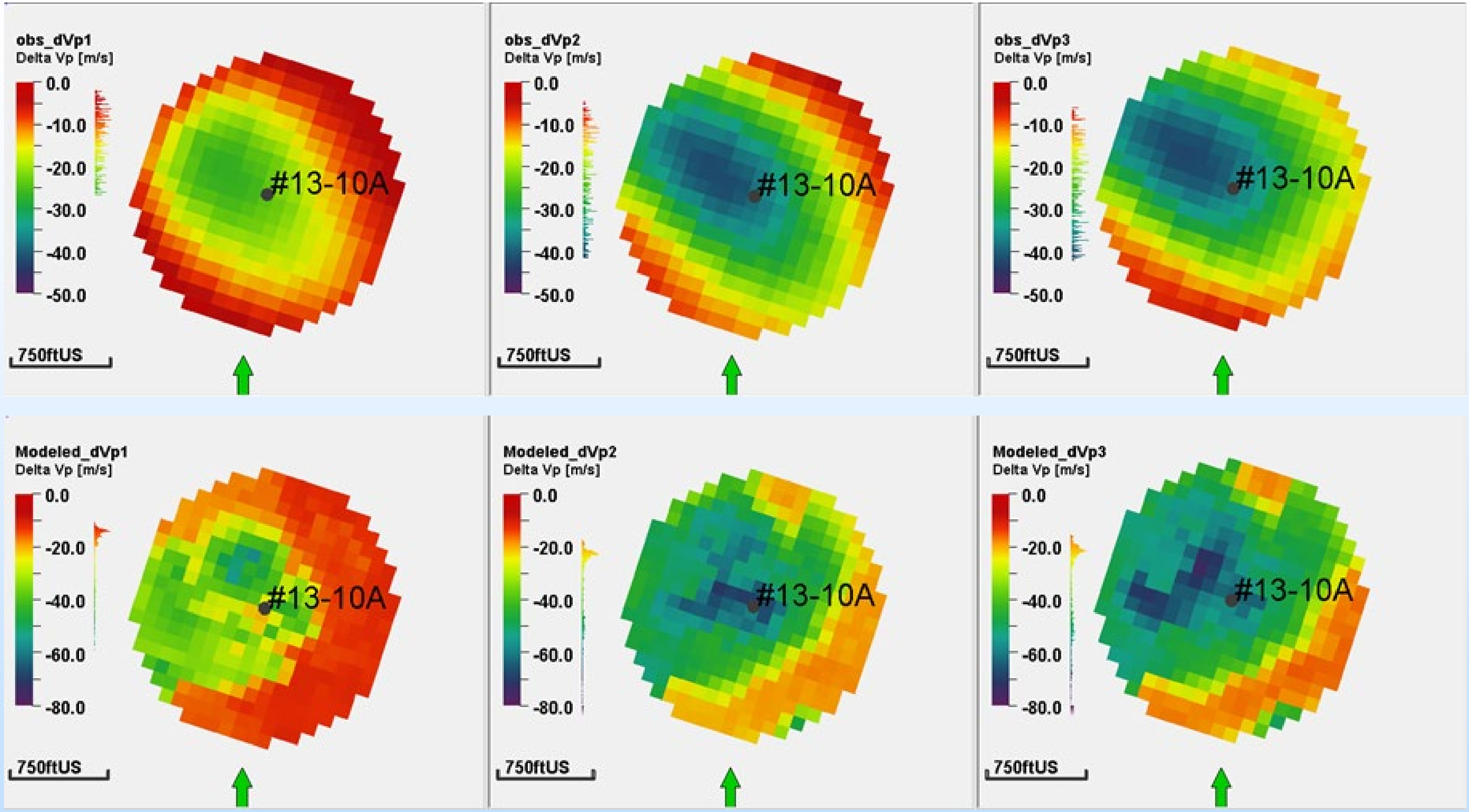

Time-Lapse Compressional Seismic Velocity Changes. Row 1 presents the observed dataset, and Row 2 represents the modeled compressional seismic velocity.

Technical Approach/Project Scope

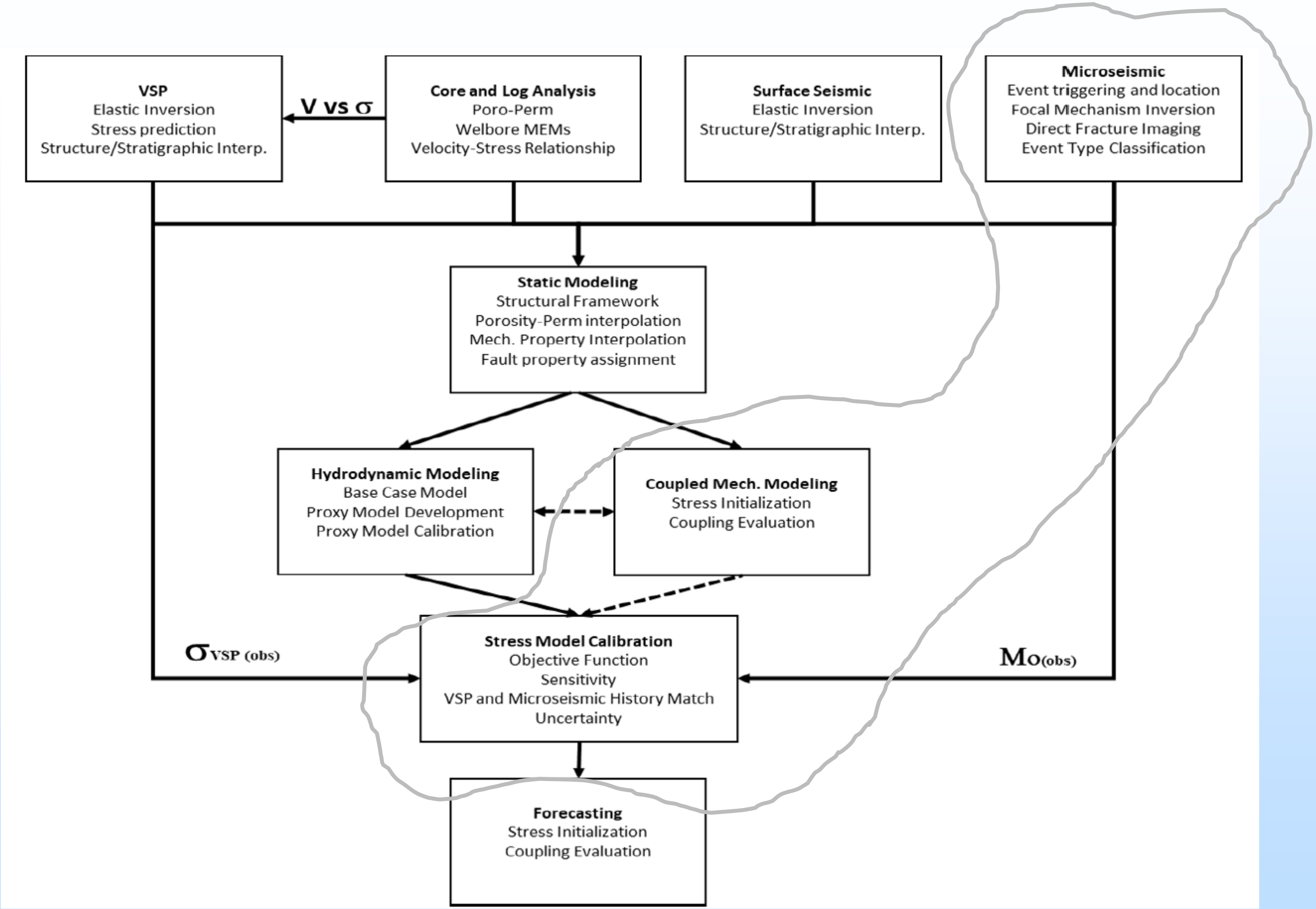

Microseismic Monitoring at Farnsworth

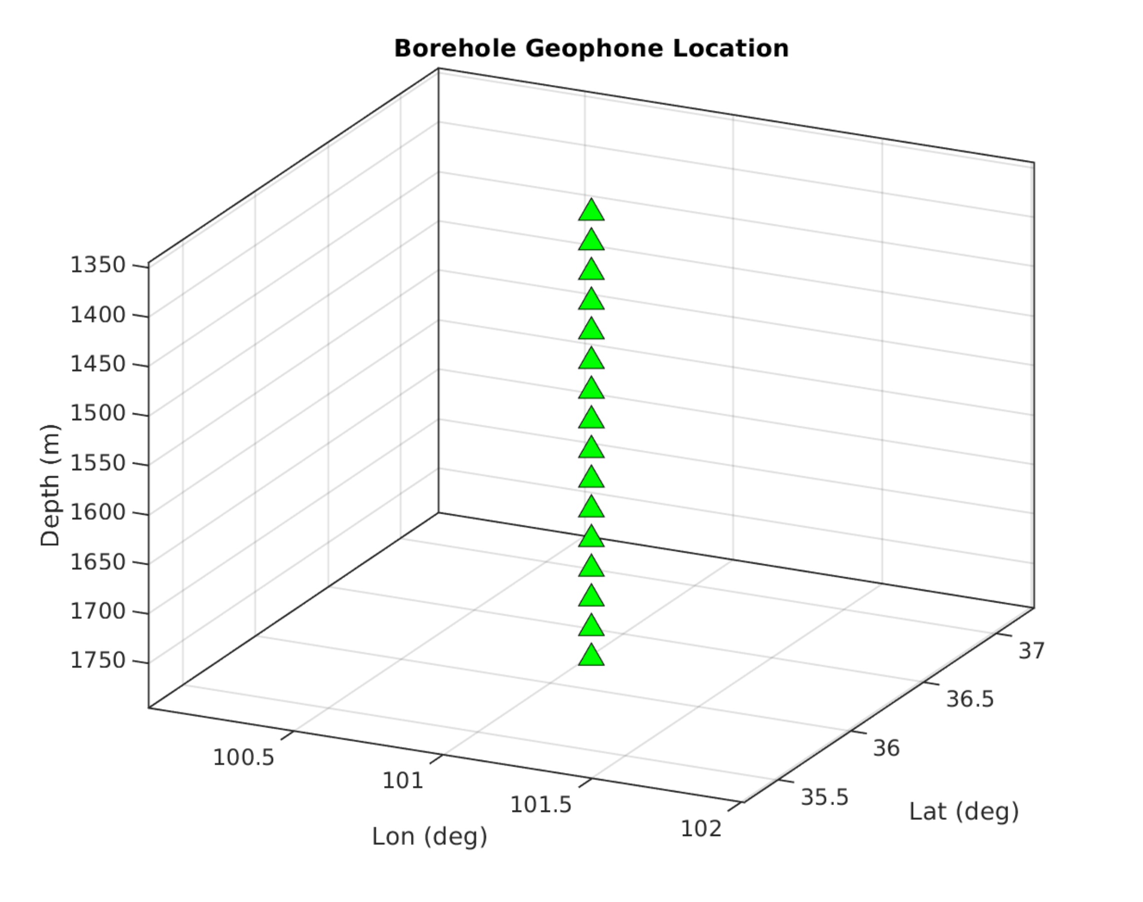

Microseismic Monitoring at Farnsworth

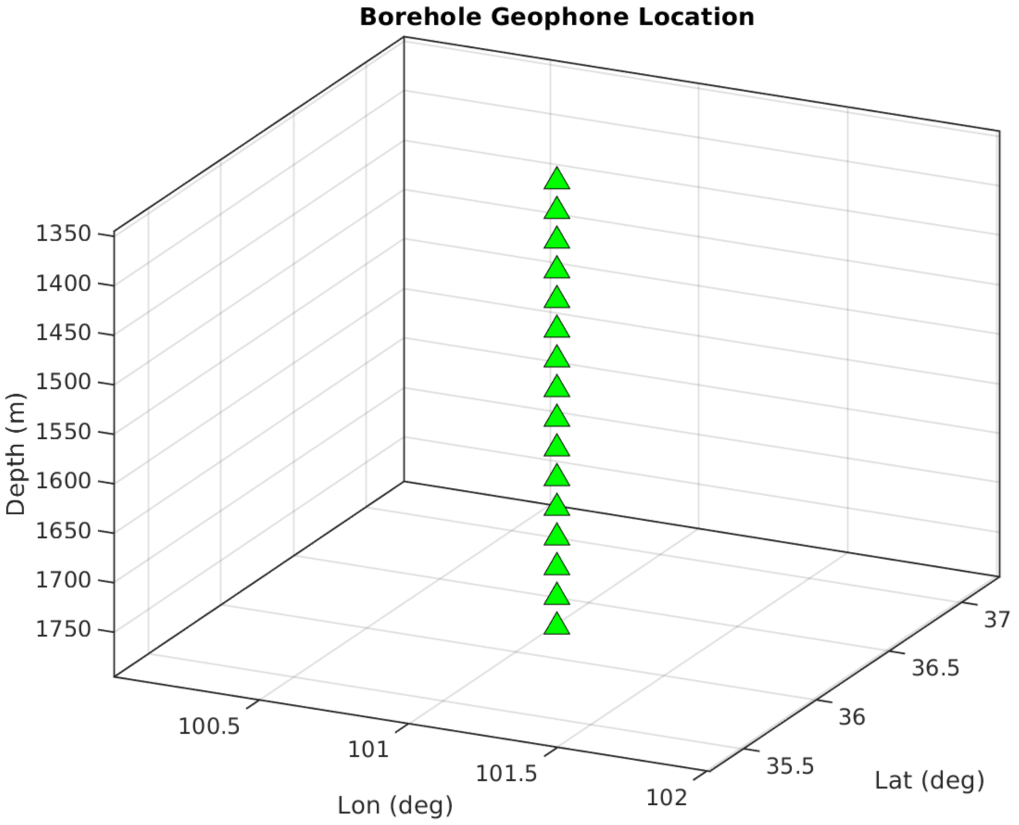

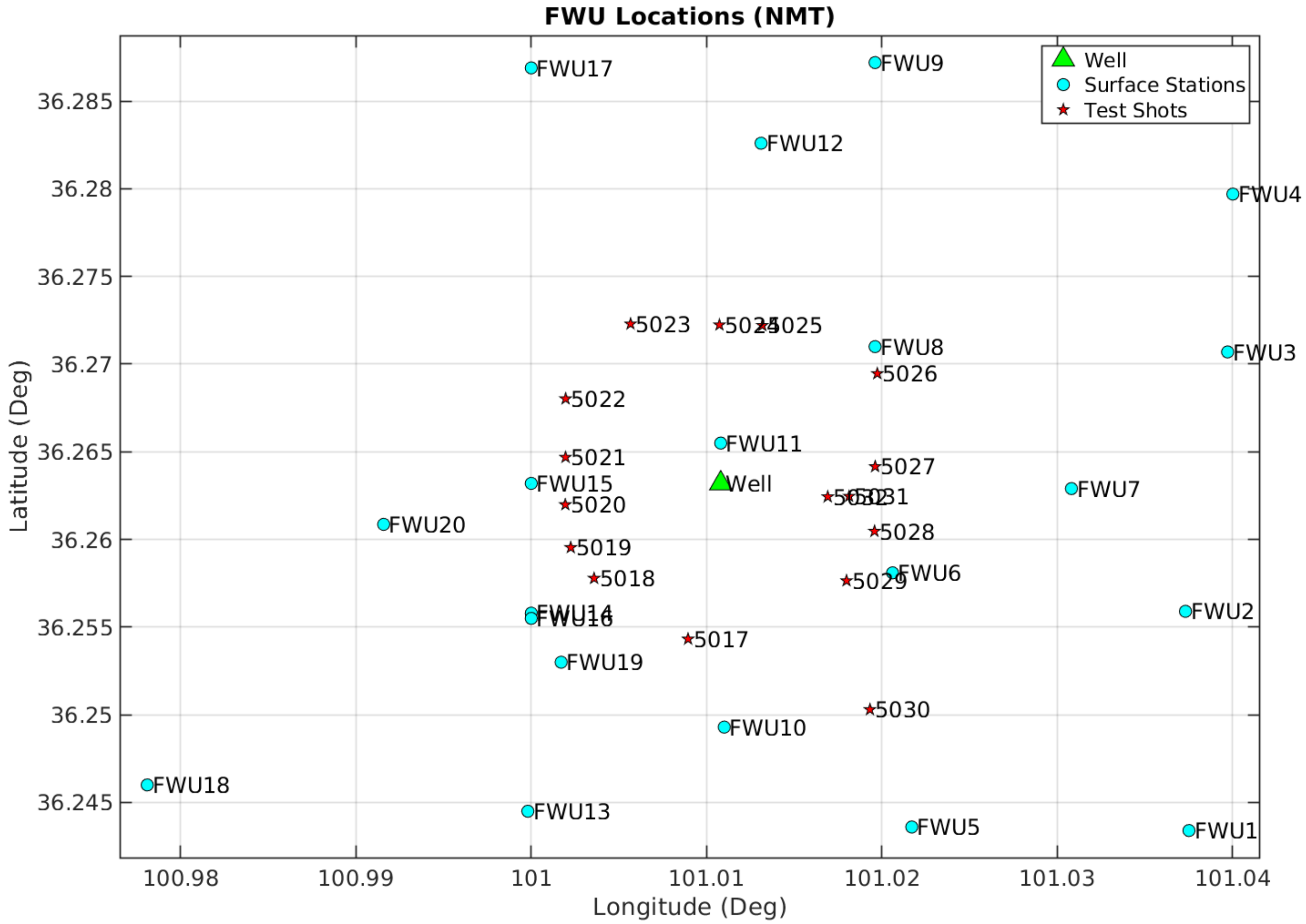

Geophone rotation using check-shot VSP data

Orientation of H1 = $\phi + (180 - \theta)$

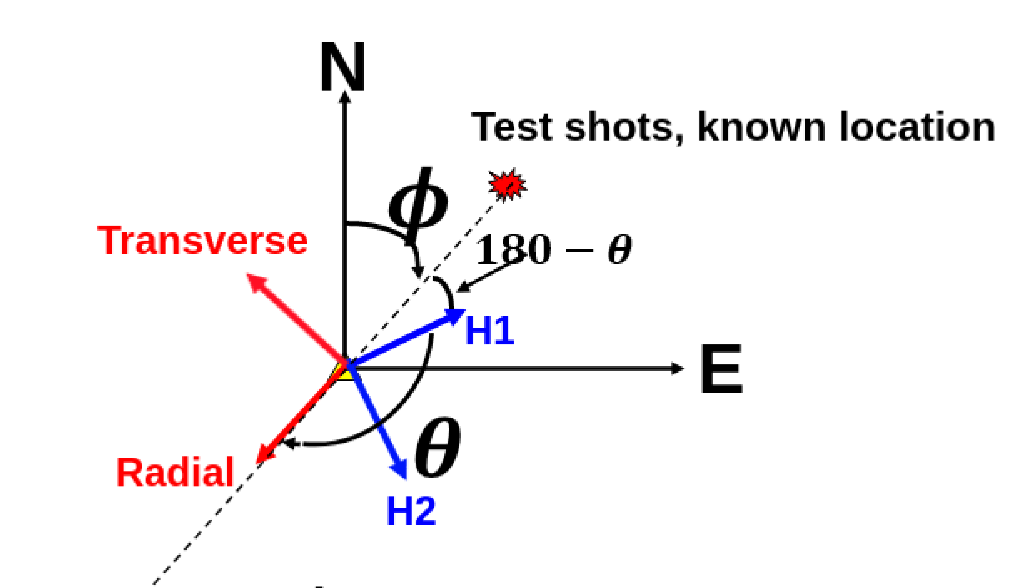

ϕ = azimuth of source to receiver

θ = rotation angle from hodogram analysis to rotate H1 to the radial direction

Orientations for 16 geophones

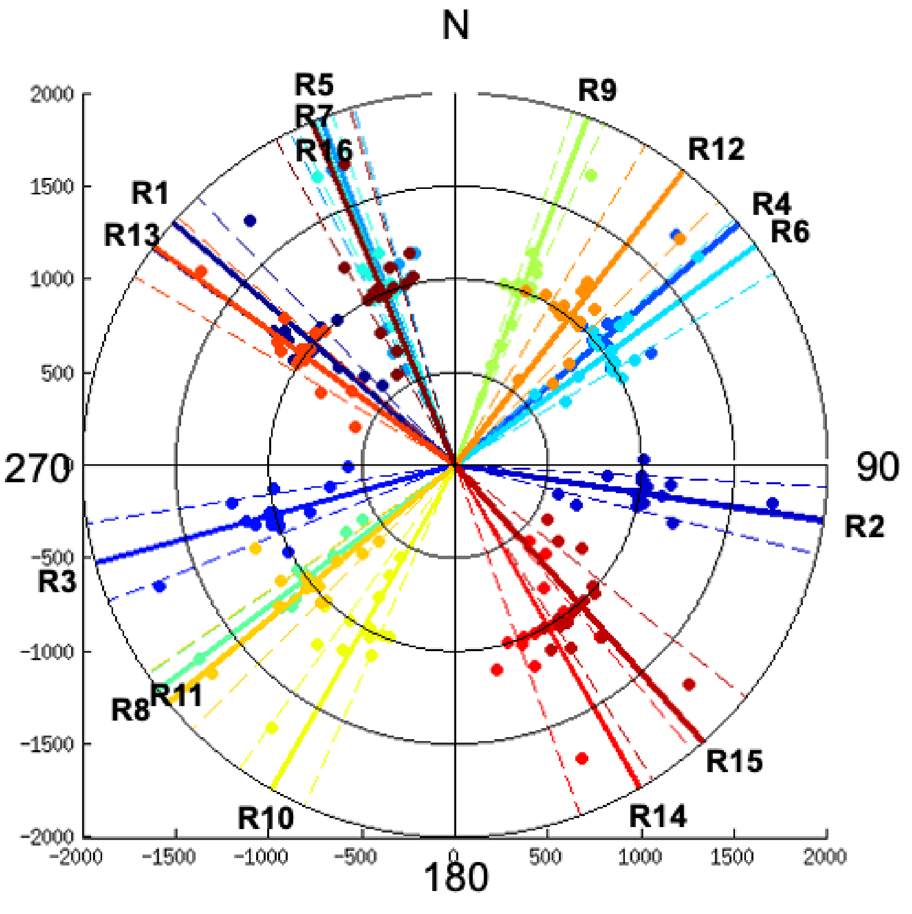

Waveform Denoising

Method: synchrosqueezed continuous wavelet transform (Mousavi et al., 2016)

Low frequency: normalization

High frequency: soft thresholding

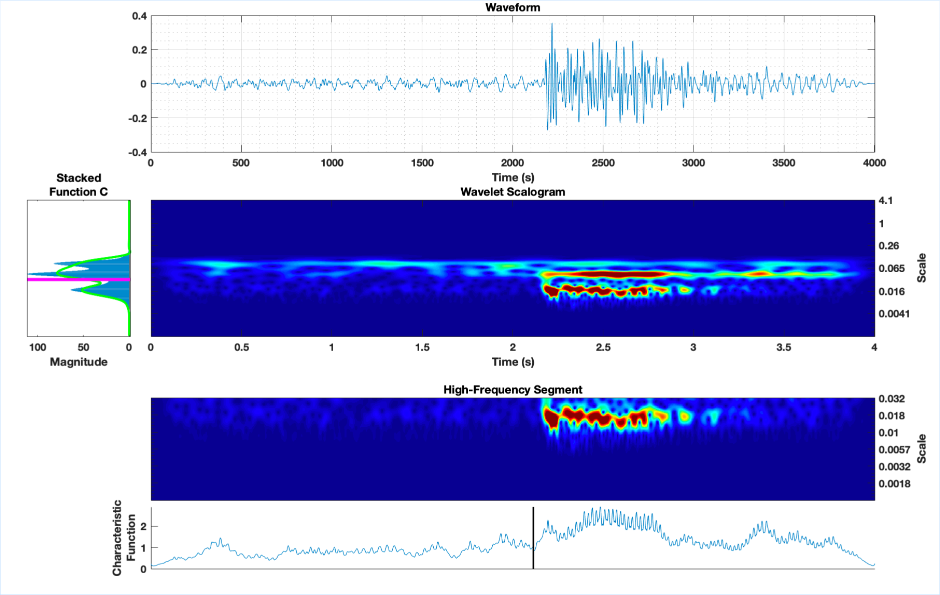

SNR comparison before and after denoising

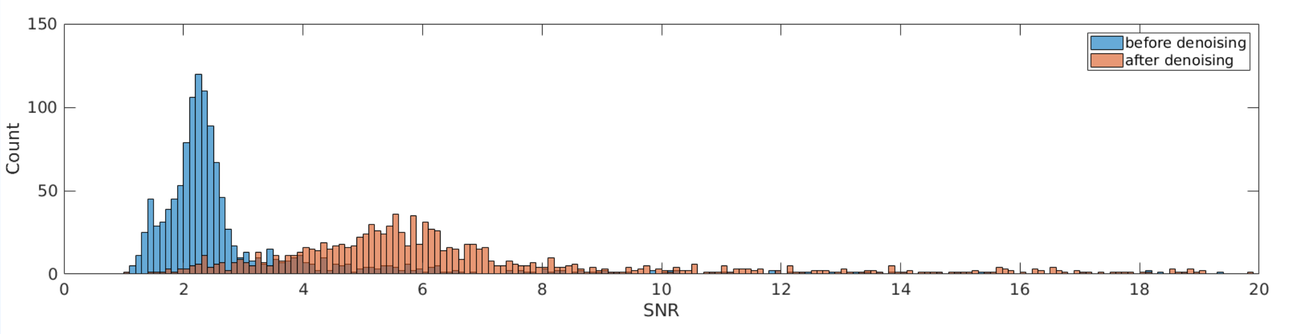

Waveform comparison before and after denoising

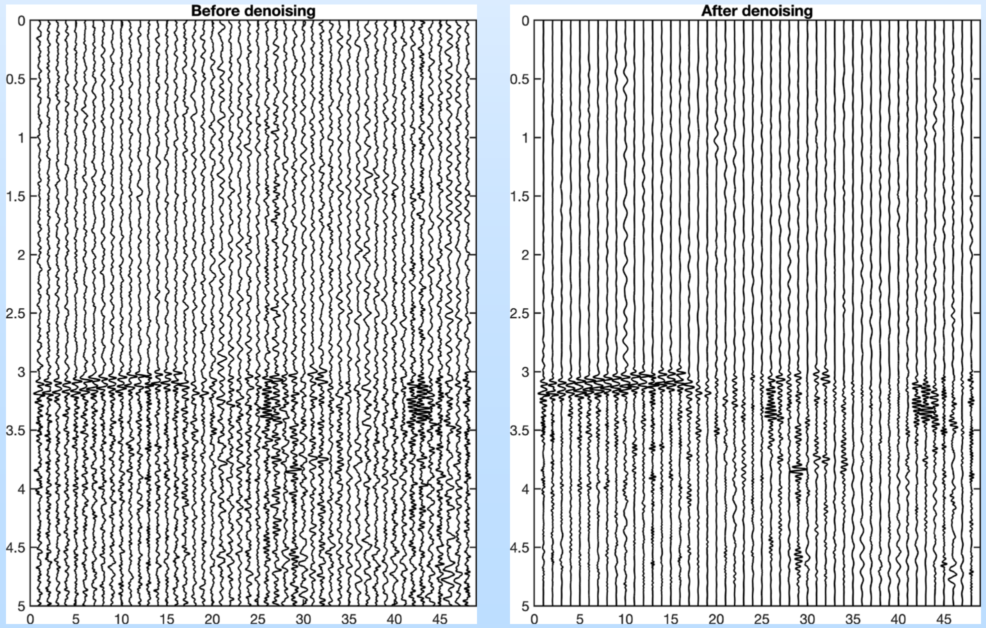

Microseismic detection using STA/LTA

An STA/LTA example

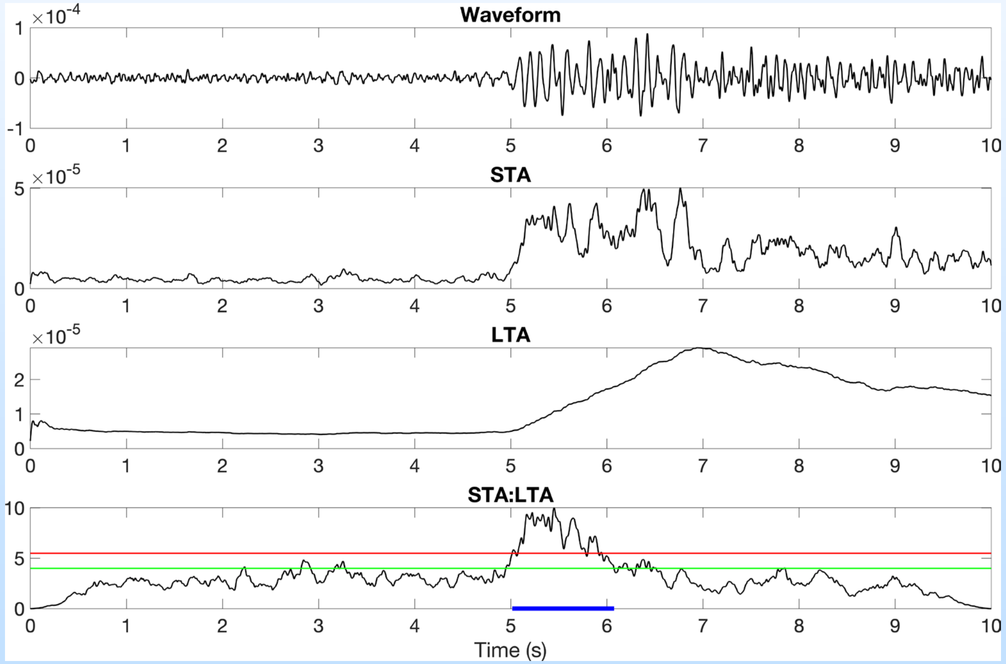

Detection results
(2020.01--2021.06)

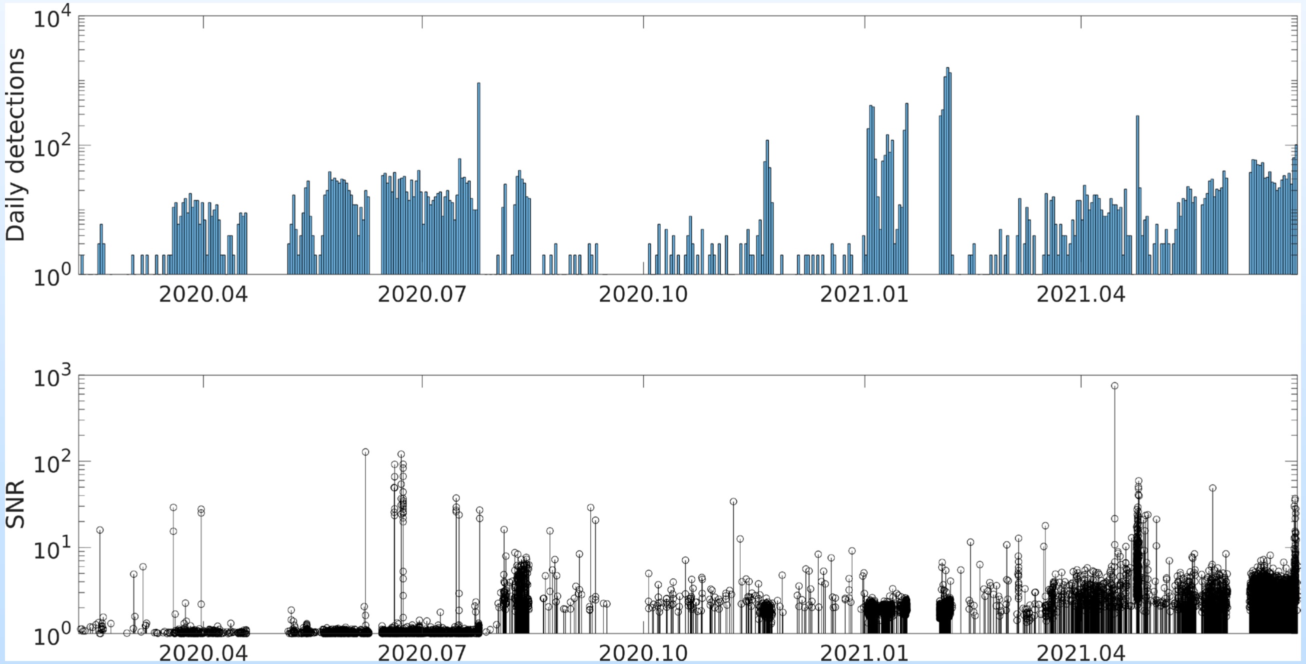

Event Location Results

- Shallow cluster, strike -57°, dip 83°
- Scattered events at depth, migration to basement

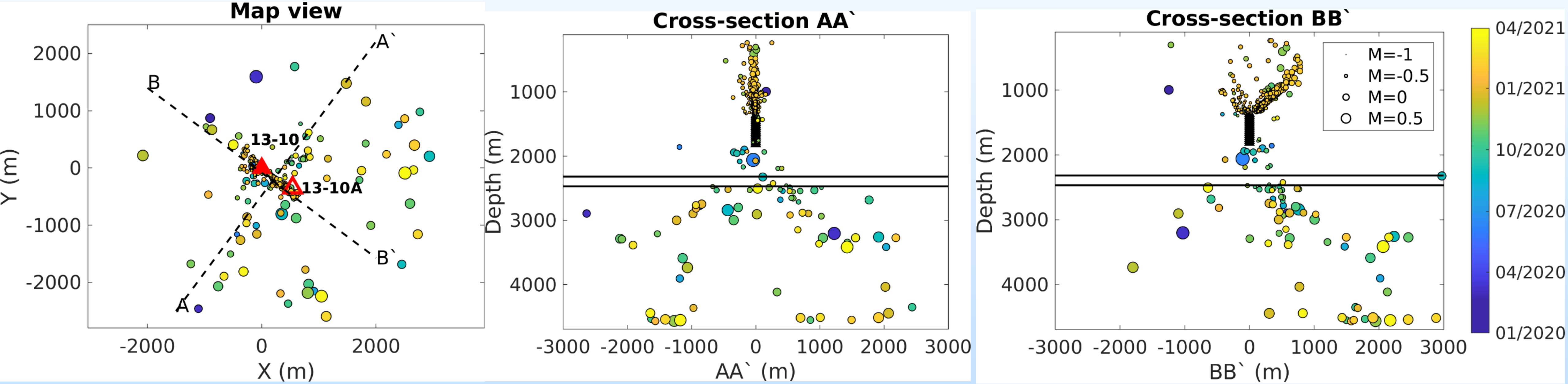

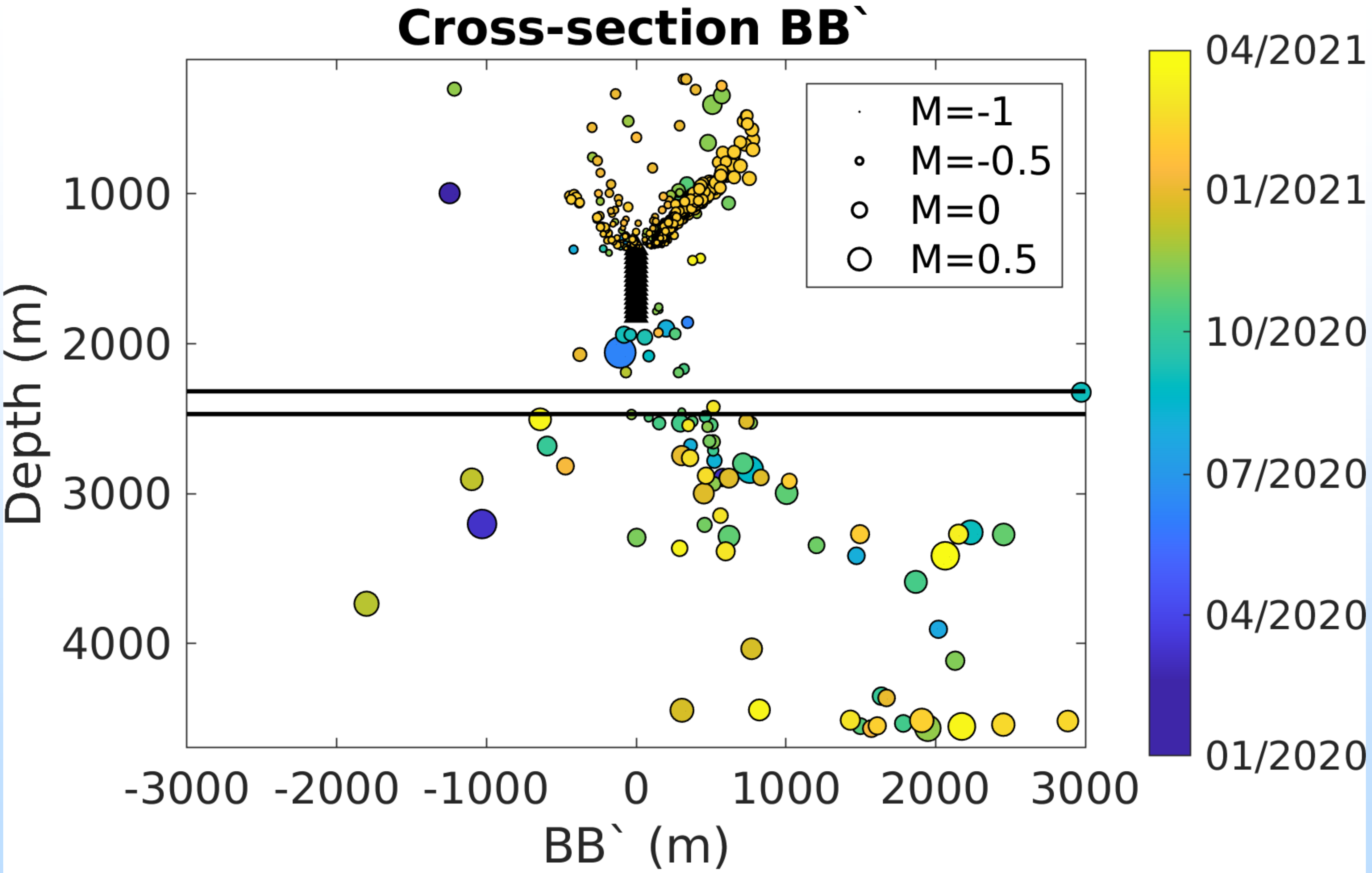
Cross-section BB`
Depth (m)
1000
2000
3000
4000
-3000
-2000
-1000
0
1000
2000
3000
BB` (m)
M=-1
M=-0.5
M=0
M=0.5
04/2021
01/2021
10/2020
07/2020
04/2020
01/2020

Moment magnitude estimation

Method: Finding the best fit long-period spectra level and corner frequency to obtain scaler seismic moment

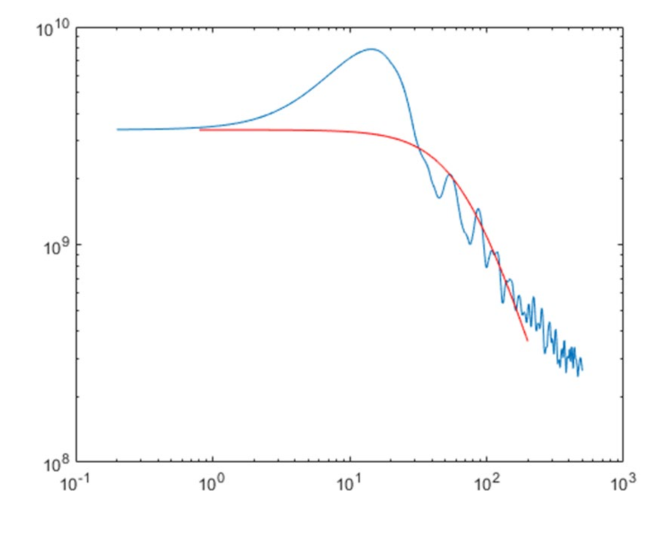

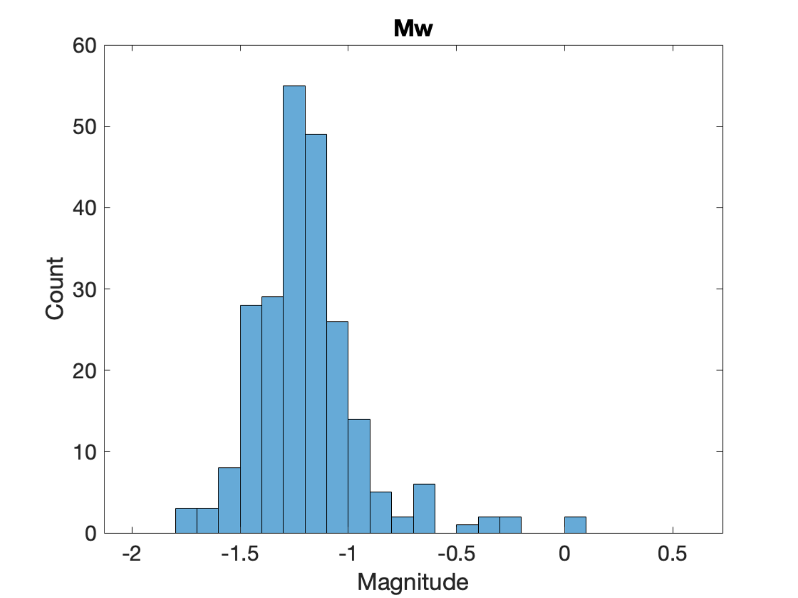

High-frequency events (2019.07—2020.02)

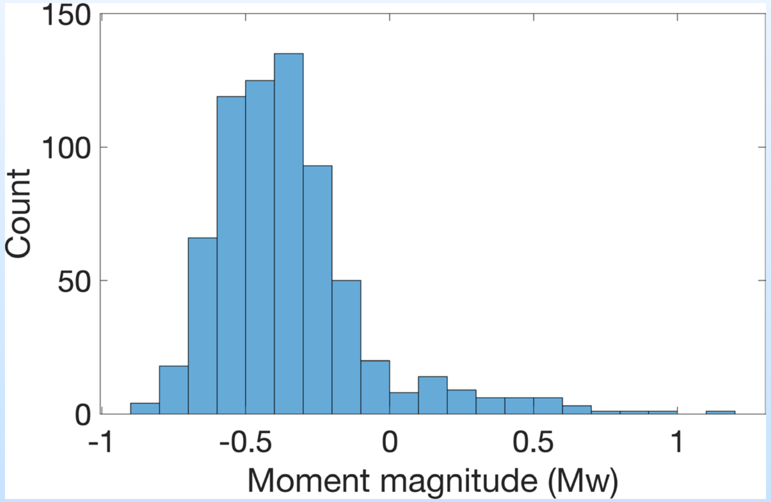

Low-frequency events (2020.01—2021.06)

Moment tensor inversion results

Using LANL's newly developed adaptive moment-tensor inversion method based on a weighted, normalized deconvolution misfit function and a zero-lag cross-correlation misfit function (Gao et al, 2021)

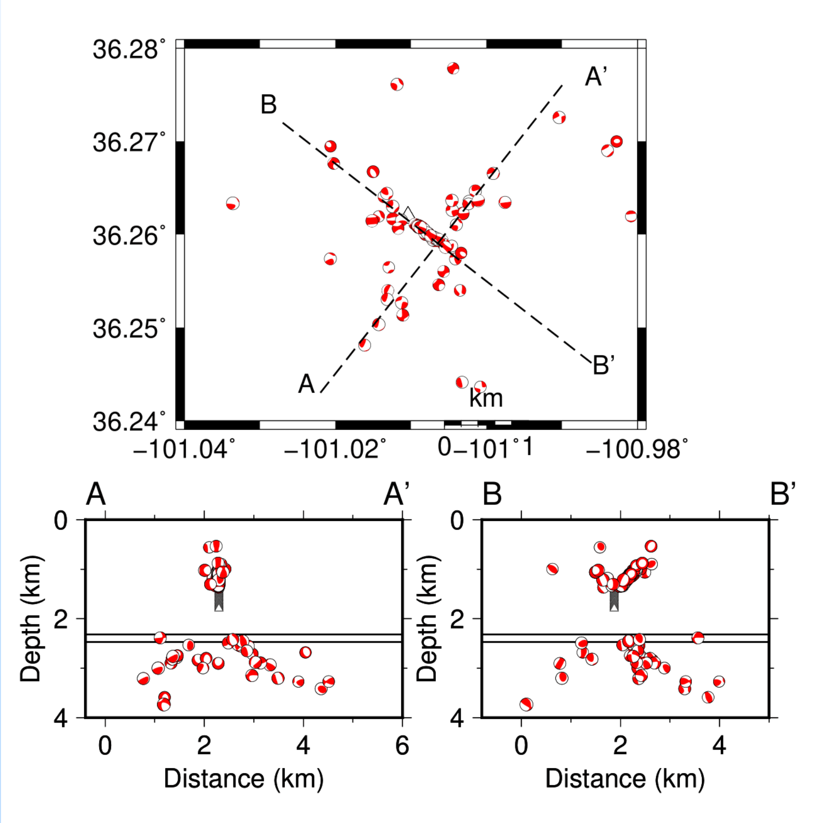

Hudson plot: Moment tensor decomposition for shallow events (<2000 m)

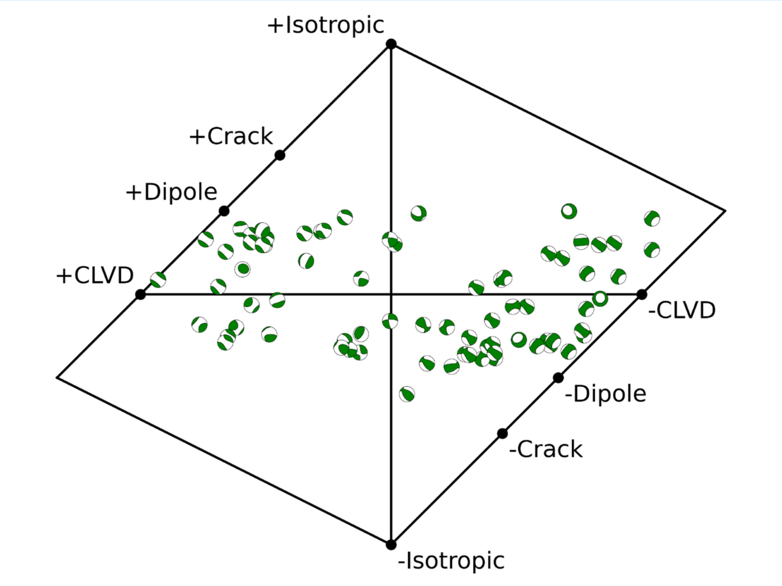

Hudson plot: Moment tensor decomposition for deep events (>2000 m); Events in the reservoir are highlighted in red.

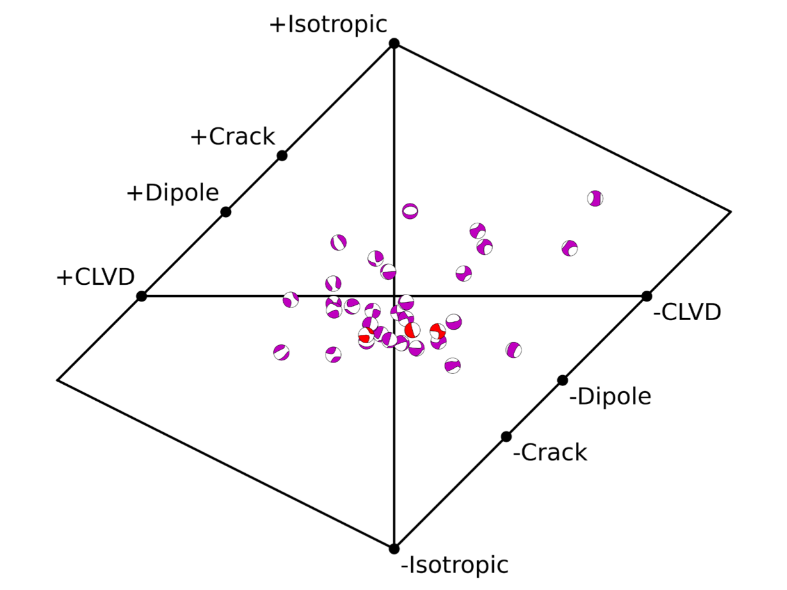

Moment tensor inversion results

- The shallow cluster corresponds to pore pressure increase and the start of gas injection; mechanism – tensile cracking (large CLVD component)
- Deeper events: Shear; CLVD component does not change over time, consistently low

Microseismicity vs injection

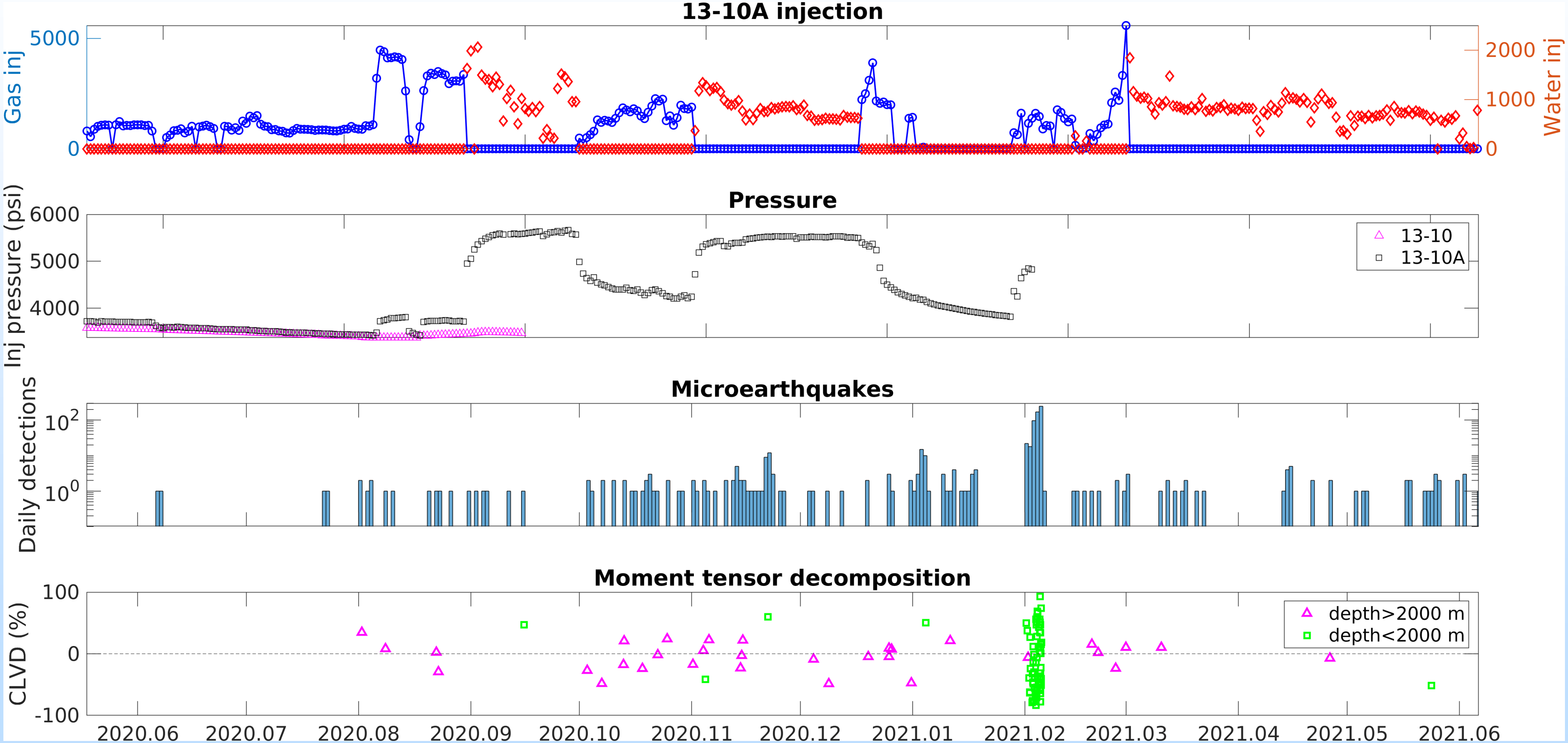

Section Objective

- Confirm microseismic event(s) can be modeled using the VSP constrained stress field from previous work
- Develop Petrel workflow to automate process and obtain objective function

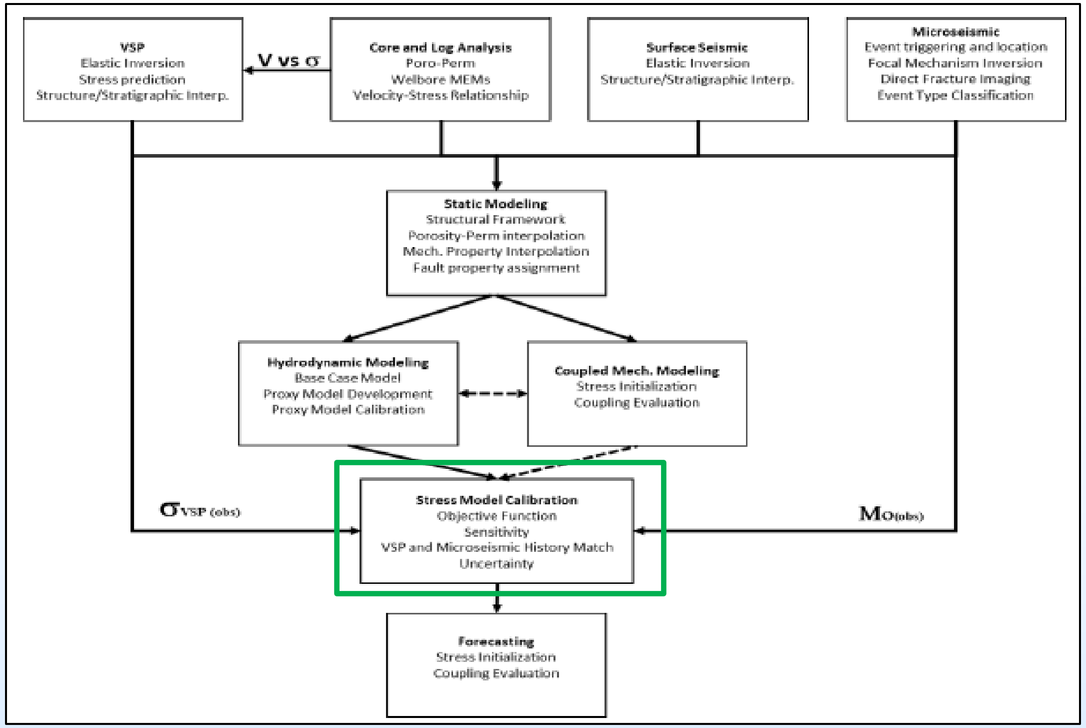

Approach

- Use microseismic events in the Morrow B and step through the process to compare model vs observed moment magnitude Mw
- 4 groups were used to prioritize analysis – initial focus on Group 1

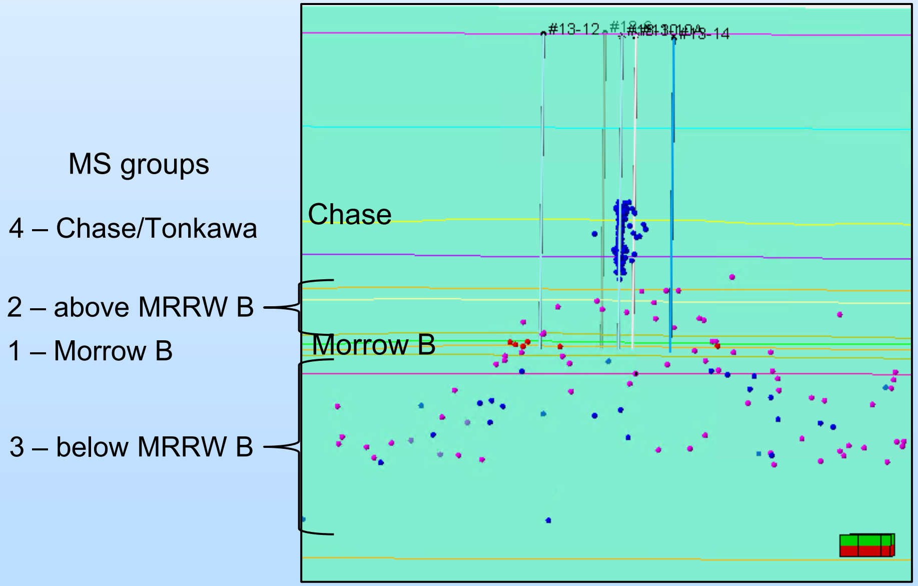

Location, timing, and two possible orientation outcomes for microseismic events in the Morrow B

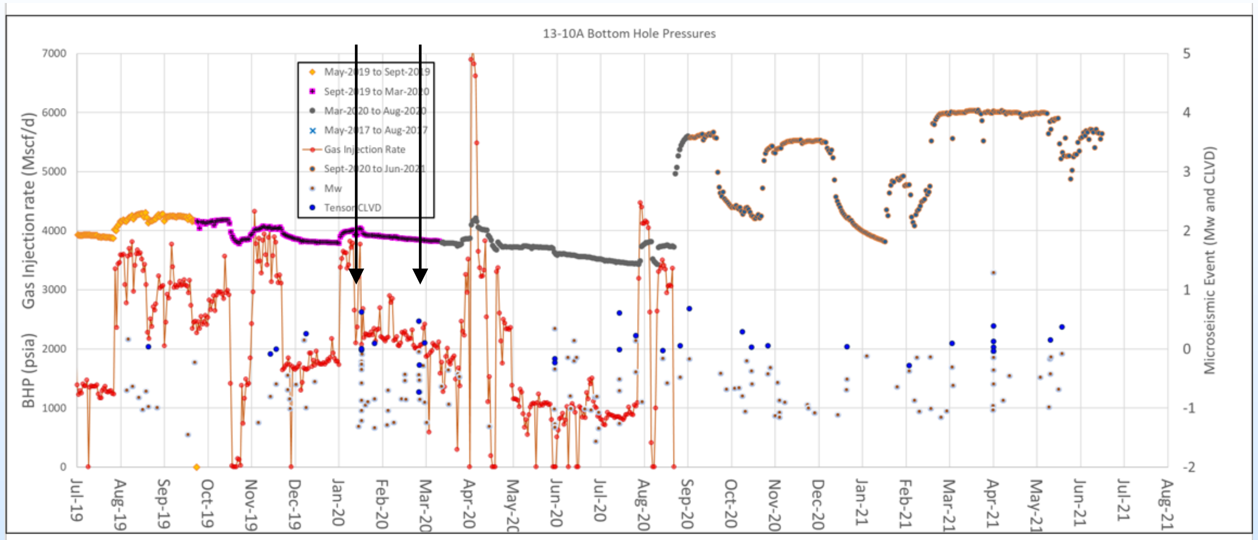

83 events (12 months 7/m)

53 events (9 months 6/m)

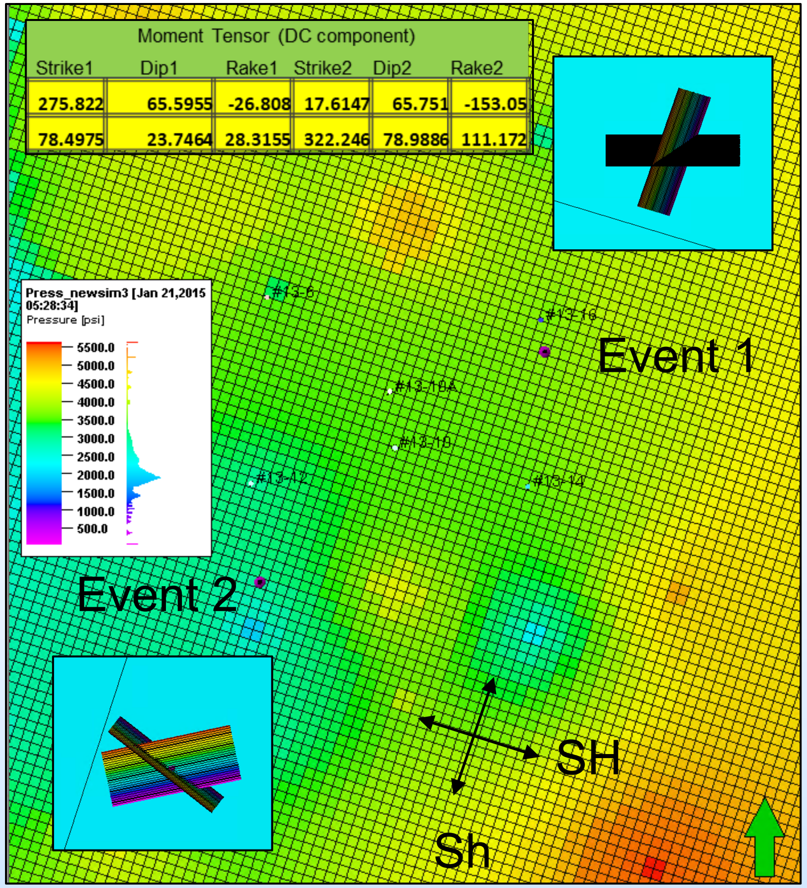

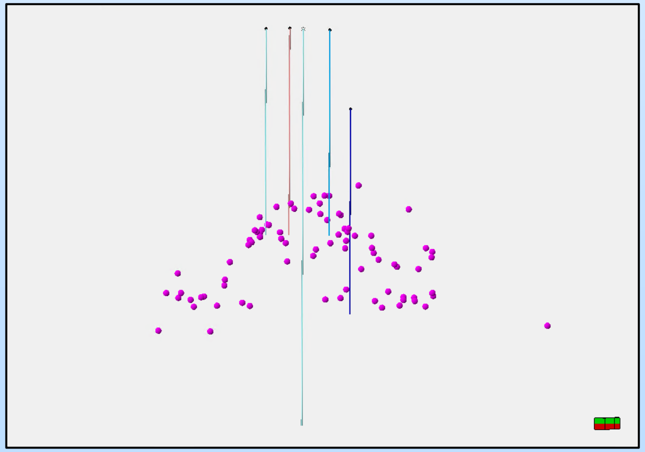

Side view

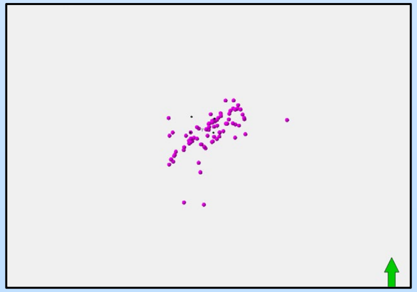

Top view

- Higher quality microseismic events needed for orientation results
- Average event count/month does not dramatically change with increasing pressure (Sep 2020)
- Events occur at increasing distance from MRRW B with increasing pressure

Location, timing, and two possible orientation outcomes for microseismic events in the Morrow B

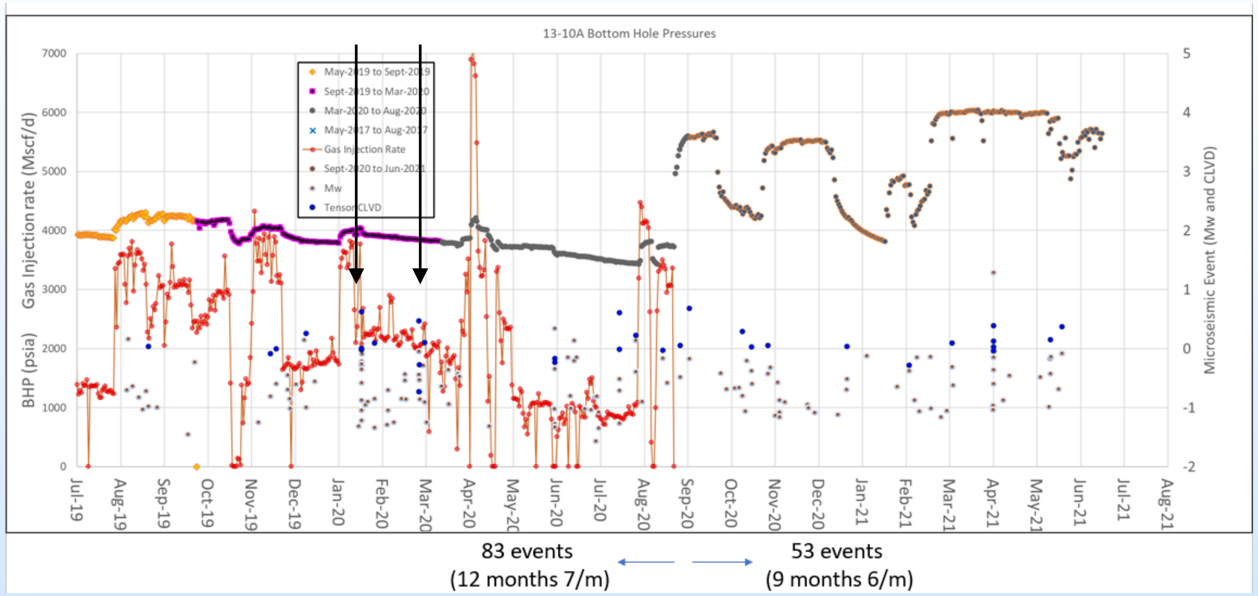

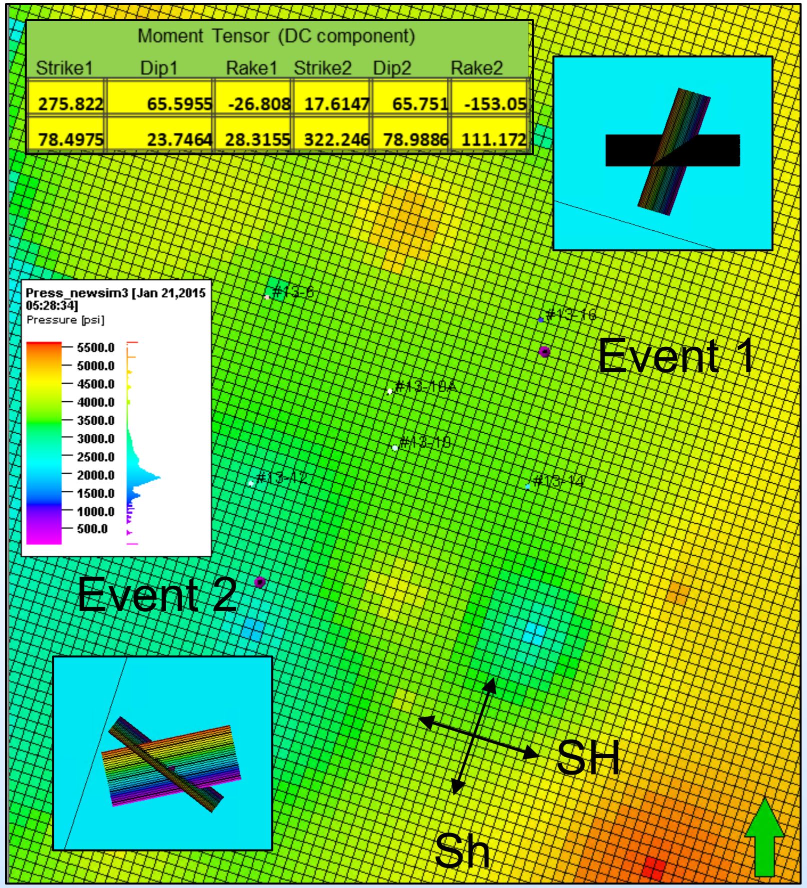

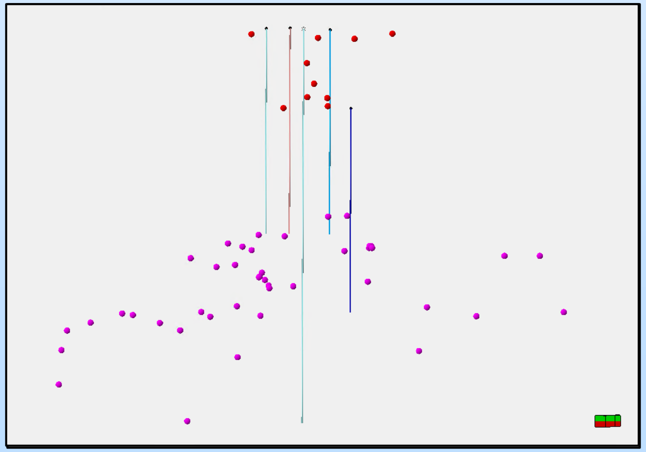

Side view

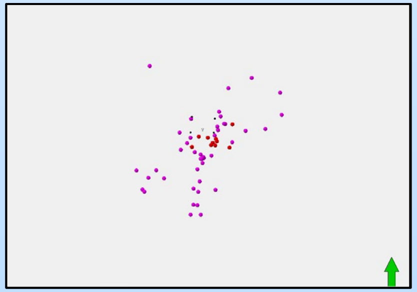

Top view

- Higher quality microseismic events needed for orientation results
- Average event count/month does not dramatically change with increasing pressure (Sep 2020)
- Events occur at increasing distance from MRRW B with increasing pressure

Model relationships and conceptual failure criteria

Model Name	Purpose	cell size (IxJ)	total cells
Geological	structural framework and properties	100x100	2.7M
Reservoir Simulation	pressure changes over time	100x100	2.7M
Main Geomechanics	regional stress state	100x100	3.4M
Sector	VSP, parameterization of fractures	100x100	2.7M
Sector 2	detail microseismic event modeling	20X20	0.651M
Sector 3	detail microseismic event modeling	20X20	1.61M

- Most events occur from small natural fractures
  - Existing fractures, not new fractures
- Events may be from opening or closing of the fractures
  - Pressure/stress increase or decrease
- The stress state is close to critical
  - Small changes in stress can produce events
- Events are non-linear
  - Failure model is plastic not elastic
  - Fracture uses a Mohr-Coulomb failure criteria
- Reverse model (not forward model)
  - Model what has happened

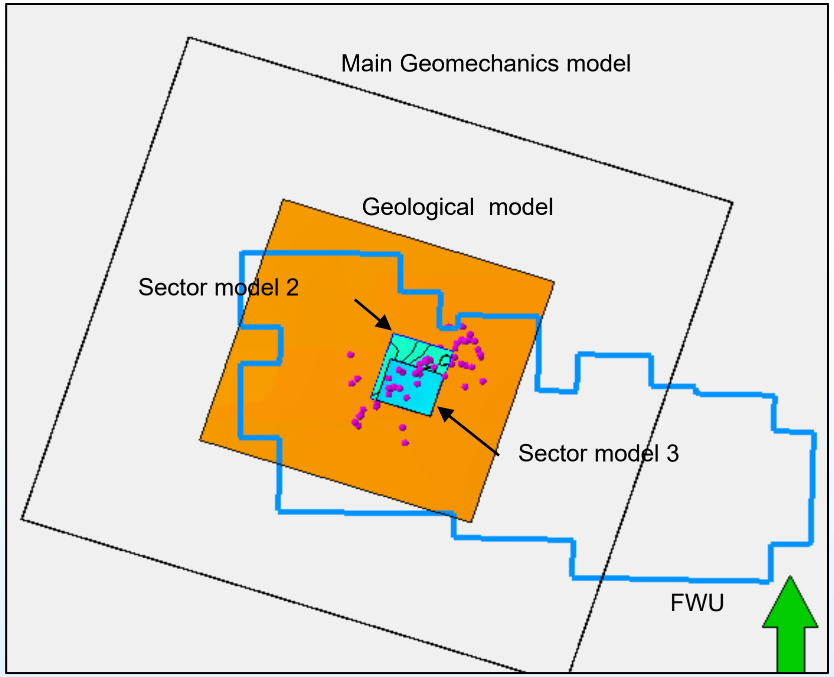

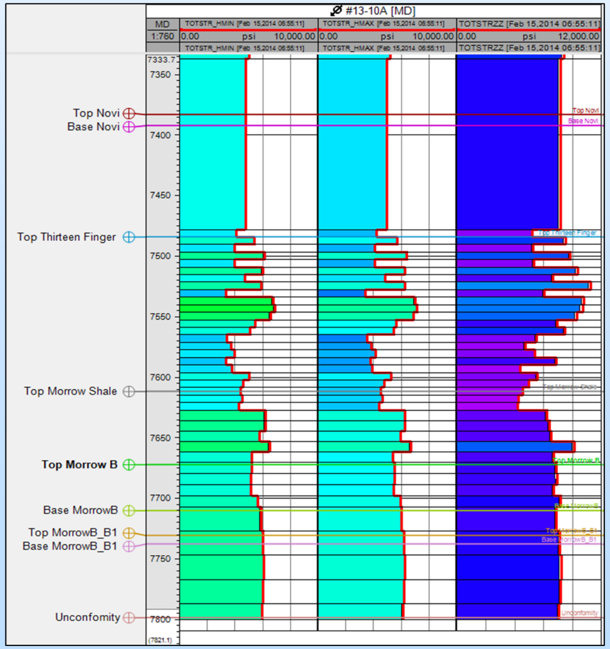

QC of sector model stress

Microseismic event with fracture plane and cells that show plastic strain

- Modeling event failure is an under-determined problem
- Parameterization analysis used to focus on key fracture properties
- Only plastic strain cells used for stress drop
- Mean stress value used for each tensor component

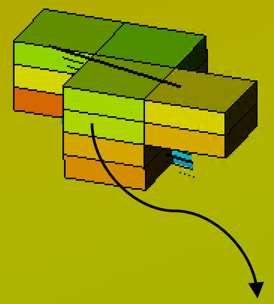

event	df22
strike	322.25
dip	78.99
u	.53
Yme_nor	.225Mpsi/ft

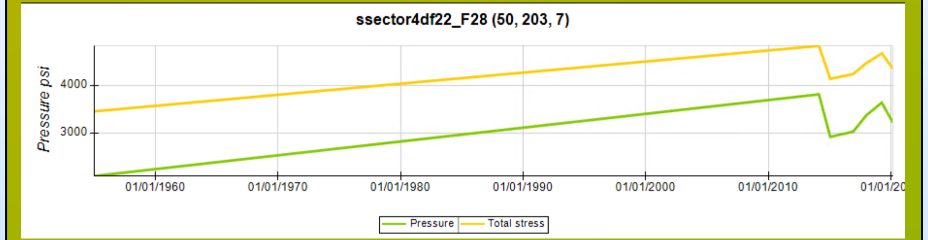

pressure and stress over time for a single cell

parameter	range	failure impact	
fracture strike (88 dip)	13, 30.5, 58, 80.5, 103	more failure towards Sh	
fracture dip (13 strike)	10, 45, 60, 75, 88	more failure in mid dips	
fracture width	40', 150'	more failure with smaller fracture	
cell size	100', 50', 20'	more failure with smaller cell	
friction coefficient (u)	.36, .58, .84, 1.19	more failure with lower u	
Ym normal/shear (K)	17/6.6, 176/66, 17000/6600	very small change	

Parametrization Analysis results
gray – small impact
yellow – medium impact
green – large impact

Name	Type	Min	Max	Delta	N	Mean	Std	Var	Sum
xxdiff22	Cont.	-9.65	127.07	136.72	11.00	77.20	39.28	1543.07	849.19
yydiff22	Cont.	-4.25	69.55	73.80	11.00	35.01	24.41	595.82	385.08
zzdiff22	Cont.	89.43	220.73	131.30	11.00	173.06	34.34	1179.40	1903.70
xydiff22	Cont.	1.38	42.45	41.07	11.00	14.12	12.41	154.00	155.33
yzdiff22	Cont.	104.11	195.97	91.85	11.00	146.97	27.18	738.86	1616.65
zxdiff22	Cont.	75.46	166.07	90.62	11.00	127.89	30.29	917.43	1406.84

Statistics for cells with plastic strain

Stress tensor to Mw results and addition of microseismic events outside of Morrow B

Stress tensor → IC,CLVD,DC → Mo,Mw

Results of Morrow B modeled Mw

Event	Observed Mw	Modeled Mw	strike (deg)	dip (deg)	coef of friction	Yme normal (Mpsi/ft)	Yme shear
1	-0.839		276	66	0.36	0.135	0.051
1	-0.839	-0.585	18	66	0.36	0.135	0.051
2	-0.433	-	79	24	0.36	0.225	0.083
2	-0.433	-0.47	322	79	0.53	0.225	0.083

- Mw magnitude is in the same range
  - Event 2 higher dip is most likely orientation
  - Either event 1 orientations are possible
- Fracture parameters necessary for failure are within physical bounds
- Fine tuning of parameter selection using error minimization needed

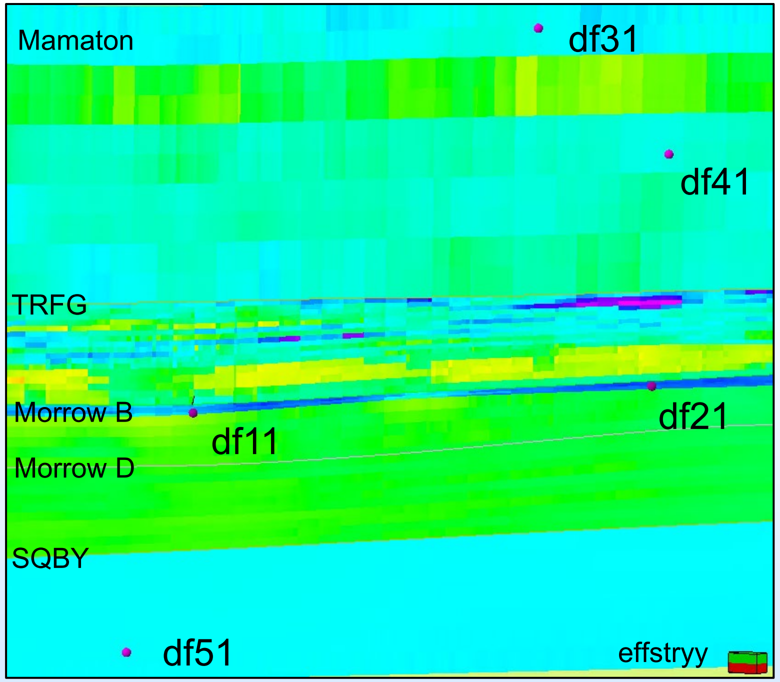

- Model events df31,df41,df51
  - Select a range of Mw events within adjacent volume
  - Create a new sector model (sector3)
  - Add additional pressure steps corresponding to event times
- Goal: to examine if pressure changes in the Morrow B will produce event occurrence from small stress changes far from the Morrow B within physical property ranges

Delta stress at df31 and modeled Mw summary

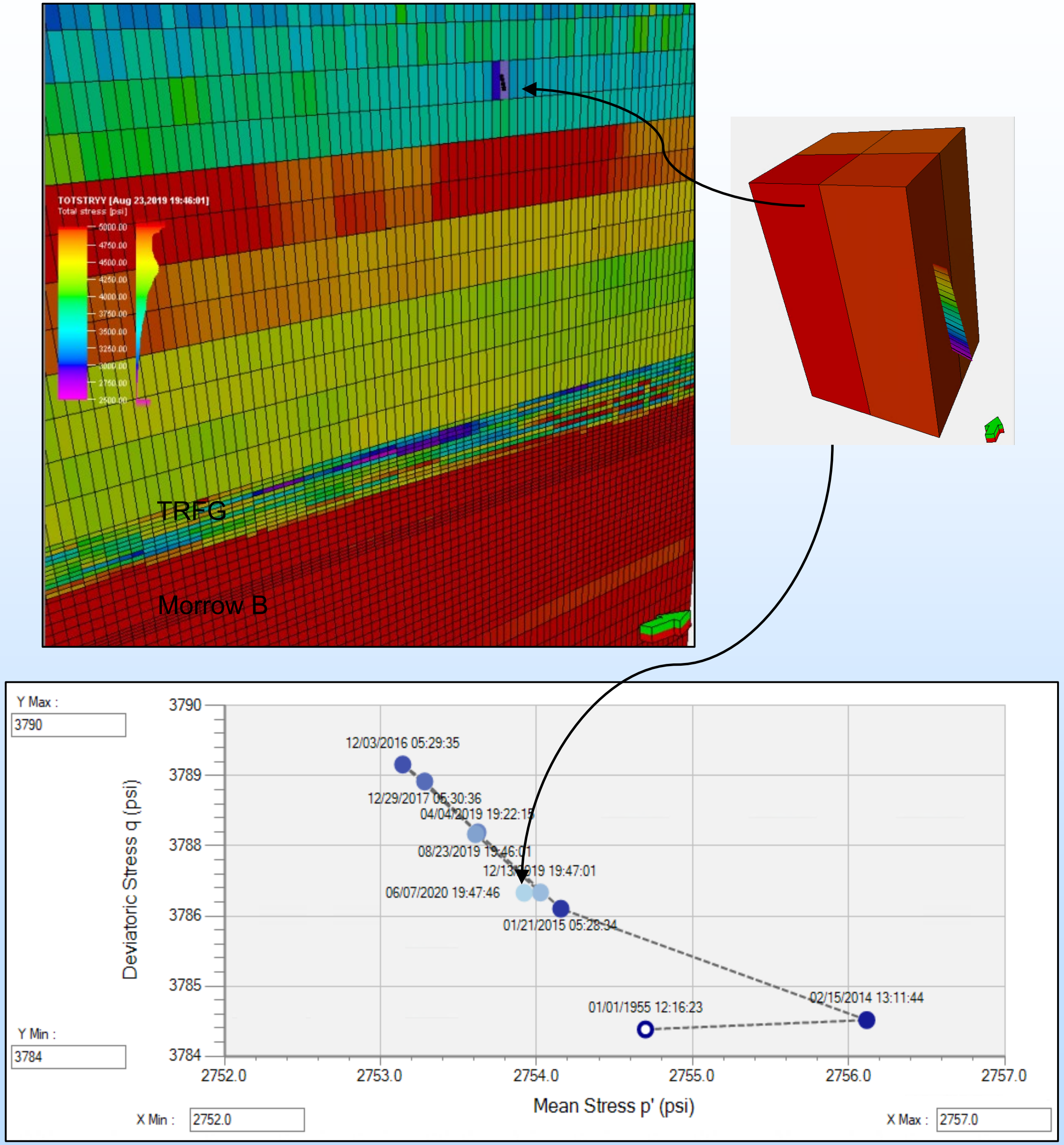

p' q plot at df3

Results of modeled Mw

Event	Observed Mw	Modeled Mw	strike (deg)	dip (deg)	coef of friction	Yme normal (Mpsi/ft)	Yme shear
1	-0.839		276	66	0.36	0.135	0.051
1	-0.839	-0.585	18	66	0.36	0.135	0.051
2	-0.433	-	79	24	0.36	0.225	0.083
2	-0.433	-0.47	322	79	0.53	0.225	0.083
3	-0.339	-1.98	131	79	0.36	0.135	0.051
4	-0.971	-2.44	94	75	0.36	0.135	0.051
5	-0.988	-2.07	108	55	0.36	0.135	0.051

- Fracture properties are within physical limits
- Modeled Mw directionally agrees with observed Mw
- Events in the Morrow B
  - Are within the same Mw magnitude
- Events outside of Morrow B
  - Have much smaller delta stress change
  - Have smaller Mw magnitude
    - Only stress change occurring outside the reservoir

Accomplishments to Date

- Completed final geological and geomechanical static models for hydrodynamic flow and coupled simulations
- Completed machine learning based VSP-Stress calibration process and forecasting
- We have applied the synchro squeezed continuous wavelet transform (SS-CWT) package (Mousavi et al., 2016) to denoise the borehole microseismic dataset from Farnsworth (2020.02—2021.06)
- Updated the event location and moment tensor inversion results using the denoised waveforms.
- Completed a manual workflow for obtaining model Mw using the Petrel workflow and python platform
- Comparison of observed Mw with modeled Mw is within the same magnitude

Summary: Key Findings/ Lessons Learned

- Higher model uncertainty exists away from the Morrow B
  - Larger cell size (more averaging of properties)
  - Less well log data below Morrow B (point df5)
  - Calibration work of previous models were all focused in the Morrow B
  - Only small stress changes occur far from the injection/production interval
- Even with model uncertainty, events were successfully modeled with similar fracture properties used for Morrow B events
- Mw magnitude is less than observed Mw for 3 new events
  - Still using the same properties as in the Morrow B with no property adjustment via error minimization
  - Magnitude trends are moving in the same direction
- Results suggest continued modeling of events away from the Morrow B calibration area would be useful in understanding the complex stress field

Next Steps

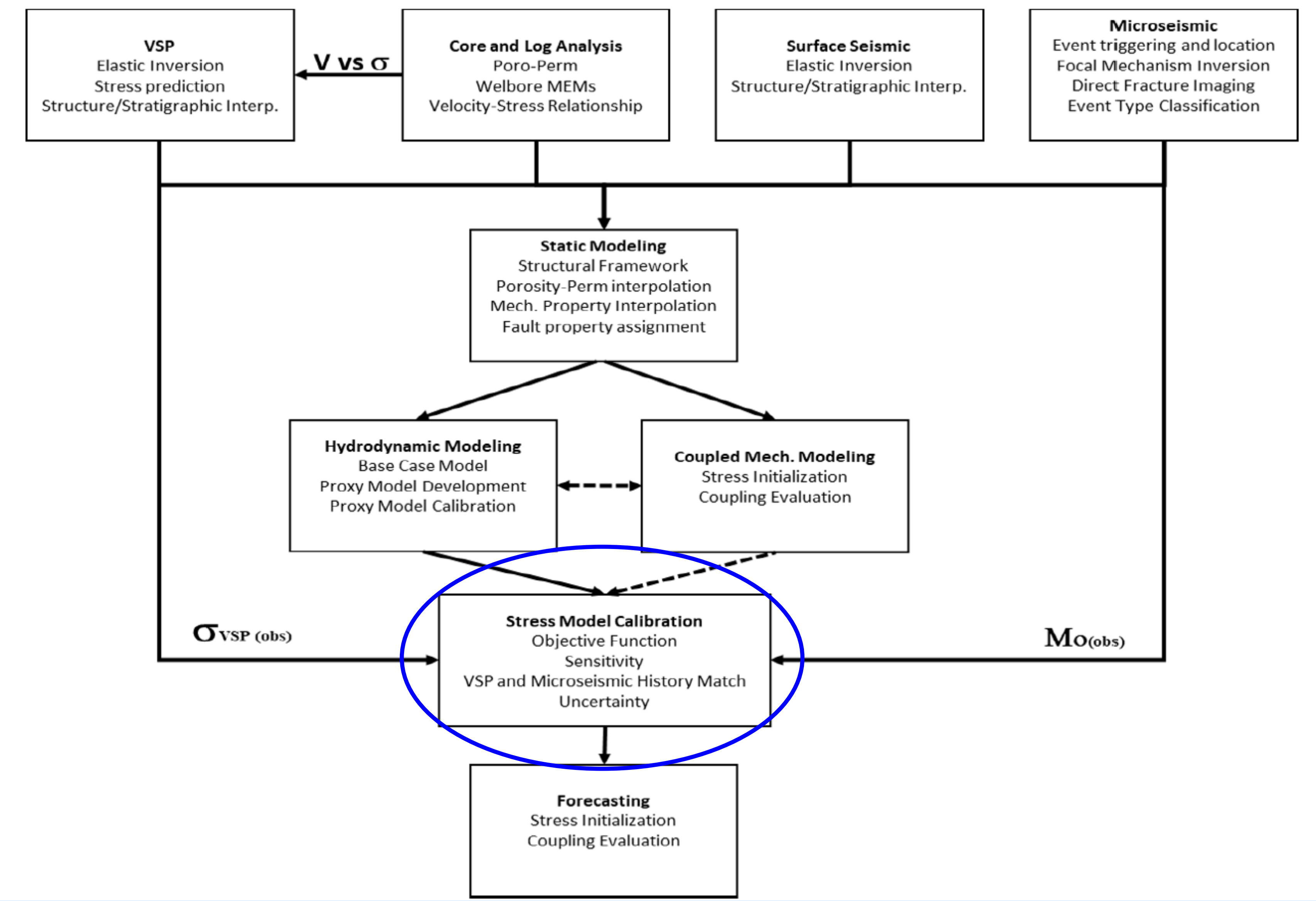
VSP
Elastic Inversion
Stress prediction
Structure/Stratigraphic Interp.
V vs σ
Core and Log Analysis
Poro-Perm
Welbore MEMs
Velocity-Stress Relationship
Surface Seismic
Elastic Inversion
Structure/Stratigraphic Interp.
Microseismic
Event triggering and location
Focal Mechanism Inversion
Direct Fracture Imaging
Event Type Classification
Static Modeling
Structural Framework
Porosity-Perm interpolation
Mech. Property Interpolation
Fault property assignment
Hydrodynamic Modeling
Base Case Model
Proxy Model Development
Proxy Model Calibration
Coupled Mech. Modeling
Stress Initialization
Coupling Evaluation
σVSP (obs)
Mo(obs)
Stress Model Calibration
Objective Function
Sensitivity
VSP and Microseismic History Match
Uncertainty
Forecasting
Stress Initialization
Coupling Evaluation

Thank you for your attention!

Organization Chart

New Mexico Tech - Prime Contract

PRRC - Project Management, (Tasks 1-8)
Ampomah - PI
Balch - Project Manager, Co-PI
Czoski, Will, El-Kaseeh, RAs
EES - Axen - Fault kinematics (Tasks 4-8)

Los Alamos National Laboratory

Huang (Co-PI) - Seismic imaging, inversion (Tasks 1-3, 8)

Sandia National Laboratory

Draelos - Machine Learning (Tasks 3, 5, 8)

Consultants

Rutledge - Geophysical methods, passive seismic monitoring (Tasks 2, 8)
Lee - Development of models (Tasks 4, 6, 7, 8)
Bratton - Geophysical methods, passive seismic monitoring (Tasks 2, 4, 6,7)

Gantt Chart

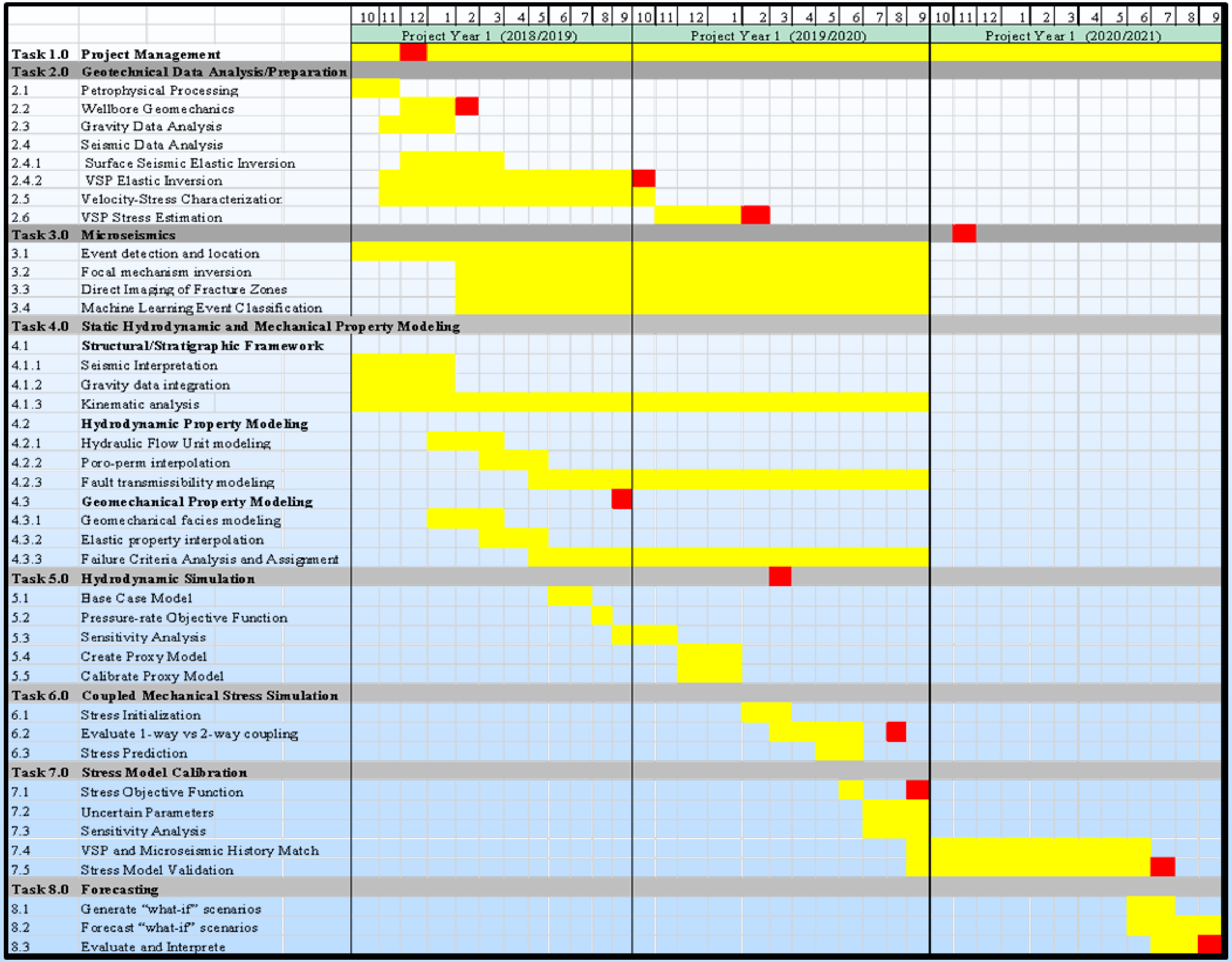

10 11 12 1 2 3 4 5 6 7 8 9 10 11 12 1 2 3 4 5 6 7 8 9 10 11 12 1 2 3 4 5 6 7 8 9
Project Year 1 (2018/2019)
Project Year 1 (2019/2020)
Project Year 1 (2020/2021)
Task 1.0 Project Management
Task 2.0 Geotechnical Data Analysis/Preparation
2.1 Petrophysical Processing
2.2 Wellbore Geomechanics
2.3 Gravity Data Analysis
2.4 Seismic Data Analysis
2.4.1 Surface Seismic Elastic Inversion
2.4.2 VSP Elastic Inversion
2.5 Velocity-Stress Characterization
2.6 VSP Stress Estimation
Task 3.0 Microseismics
3.1 Event detection and location
3.2 Focal mechanism inversion
3.3 Direct Imaging of Fracture Zones
3.4 Machine Learning Event Classification
Task 4.0 Static Hydrodynamic and Mechanical Property Modeling
4.1 Structural/Stratigraphic Framework
4.1.1 Seismic Interpretation
4.1.2 Gravity data integration
4.1.3 Kinematic analysis
4.2 Hydrodynamic Property Modeling
4.2.1 Hydraulic Flow Unit modeling
4.2.2 Poro-perm interpolation
4.2.3 Fault transmissibility modeling
4.3 Geomechanical Property Modeling
4.3.1 Geomechanical facies modeling
4.3.2 Elastic property interpolation
4.3.3 Failure Criteria Analysis and Assignment
Task 5.0 Hydrodynamic Simulation
5.1 Base Case Model
5.2 Pressure-rate Objective Function
5.3 Sensitivity Analysis
5.4 Create Proxy Model
5.5 Calibrate Proxy Model
Task 6.0 Coupled Mechanical Stress Simulation
6.1 Stress Initialization
6.2 Evaluate 1-way vs 2-way coupling
6.3 Stress Prediction
Task 7.0 Stress Model Calibration
7.1 Stress Objective Function
7.2 Uncertain Parameters
7.3 Sensitivity Analysis
7.4 VSP and Microseismic History Match
7.5 Stress Model Validation
Task 8.0 Forecasting
8.1 Generate "what-if" scenarios
8.2 Forecast "what-if" scenarios
8.3 Evaluate and Interprete

Geomechanical Calibration: Parameter Sensitivities

Task 7.2 and 7.3

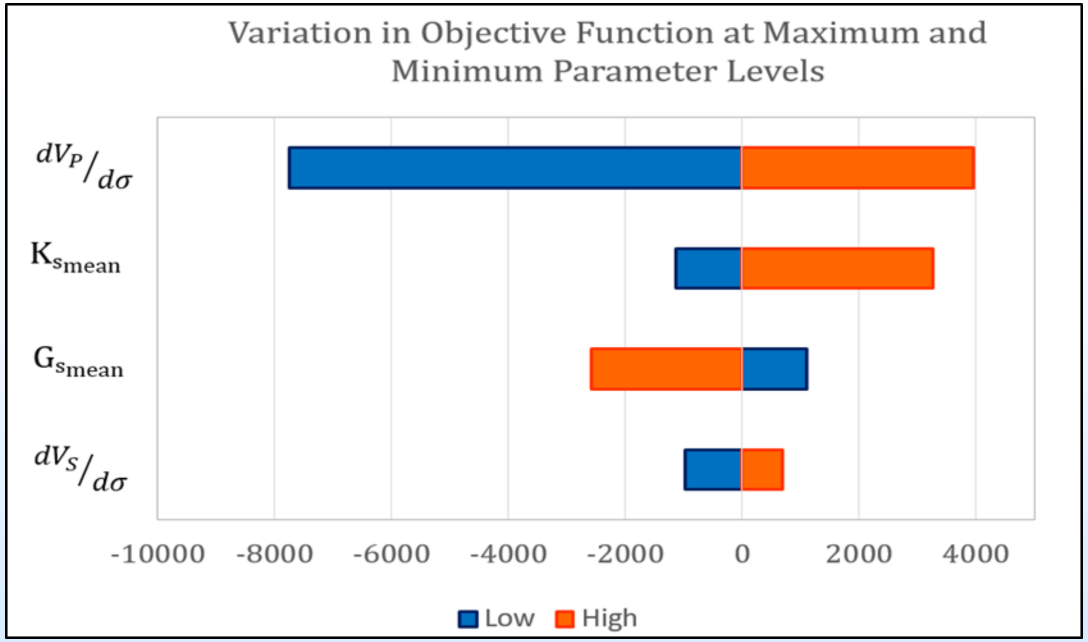

	Parameter Values		Objective Functions	
	Low	High	Low	High
Shear Modulus at Zero Porosity (Mpsi)	2.40	3.00	1108.79	-2588.53
Bulk Modulus at Zero Porosity (Mpsi)	3.00	3.90	-1137.23	3267.00
Derivative of Shear Seismic Velocity to Mean Effective Stress (m/s per 1000 psi Δ in mean effective stress)	7.00	70.00	-971.85	686.98
Derivative of Compressional Seismic Velocity to Mean Effective Stress (m/s per 1000 psi Δ in mean effective stress)	15.00	152.00	-7740.91	3946.94

- Four Independent variables control both the fluid substitution and mean effective stress impacts on shear and compressional seismic velocity changes
  - P-velocity – Mean Effective Stress Ratio
  - S-velocity – Mean Effective Stress Ratio
- Reflects the larger influence of mean effective stress changes on the Total Objective Function.
- Gs_{mean} and Ks_{mean} impacts
  - Fluid substitution: Saturated Bulk modulus and Shear Modulus
  - Mean effective stress through the linear elastic assumption.
  - Bulk Modulus incorporates the effect of fluid compressibility and saturation distribution. Shear modulus is unchanged.

Regression Analysis: Artificial Neural Network

- Artificial Neural Networks (ANN) are inspired by the structure of the Human Brain.
  - Comprised of layers of neurons that form the core processing units of the ANN
  - Weights are assigned at each layer prior to neuron activation throughout the network to generate the output(s)
  - Utilize the Backpropagation algorithm (supervised algorithm) to train ANN and update the weights until the error between the computed and simulated outputs are minimized.

- Subdivide Inputs (randomly determined)
  - Training (70%), Validation (15%), Blind Testing (15%)
  - Single hidden layer comprised of 15 neurons

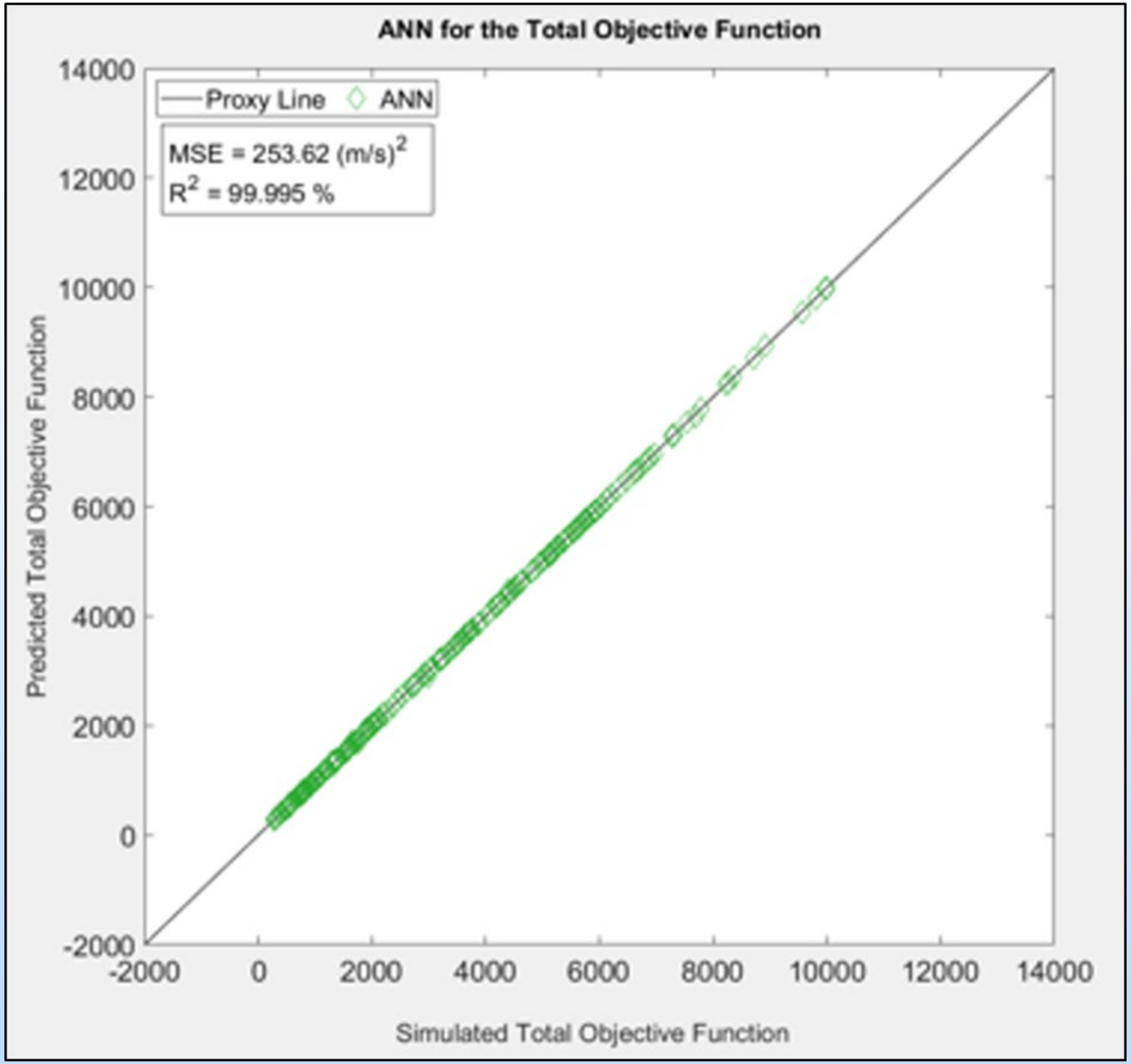

VSP- Geomechanical Calibration Task 7.4 – Baseline dVP

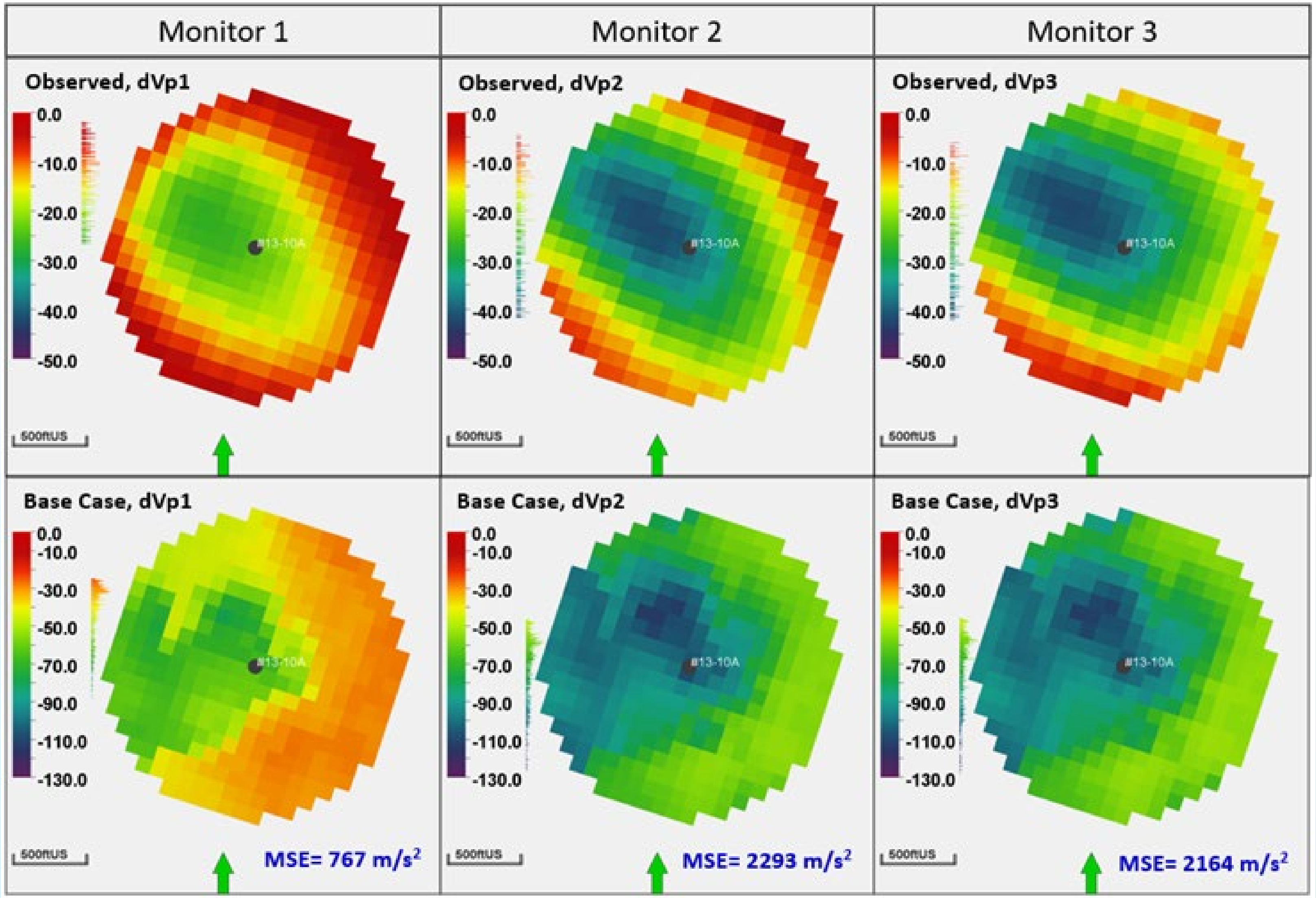

Time-Lapse Compressional Seismic Velocity Changes. Row 1 presents the observed dataset, and Row 2 represents the modeled compressional seismic velocity.

VSP- Geomechanical Calibration Task 7.4- Baseline dVs

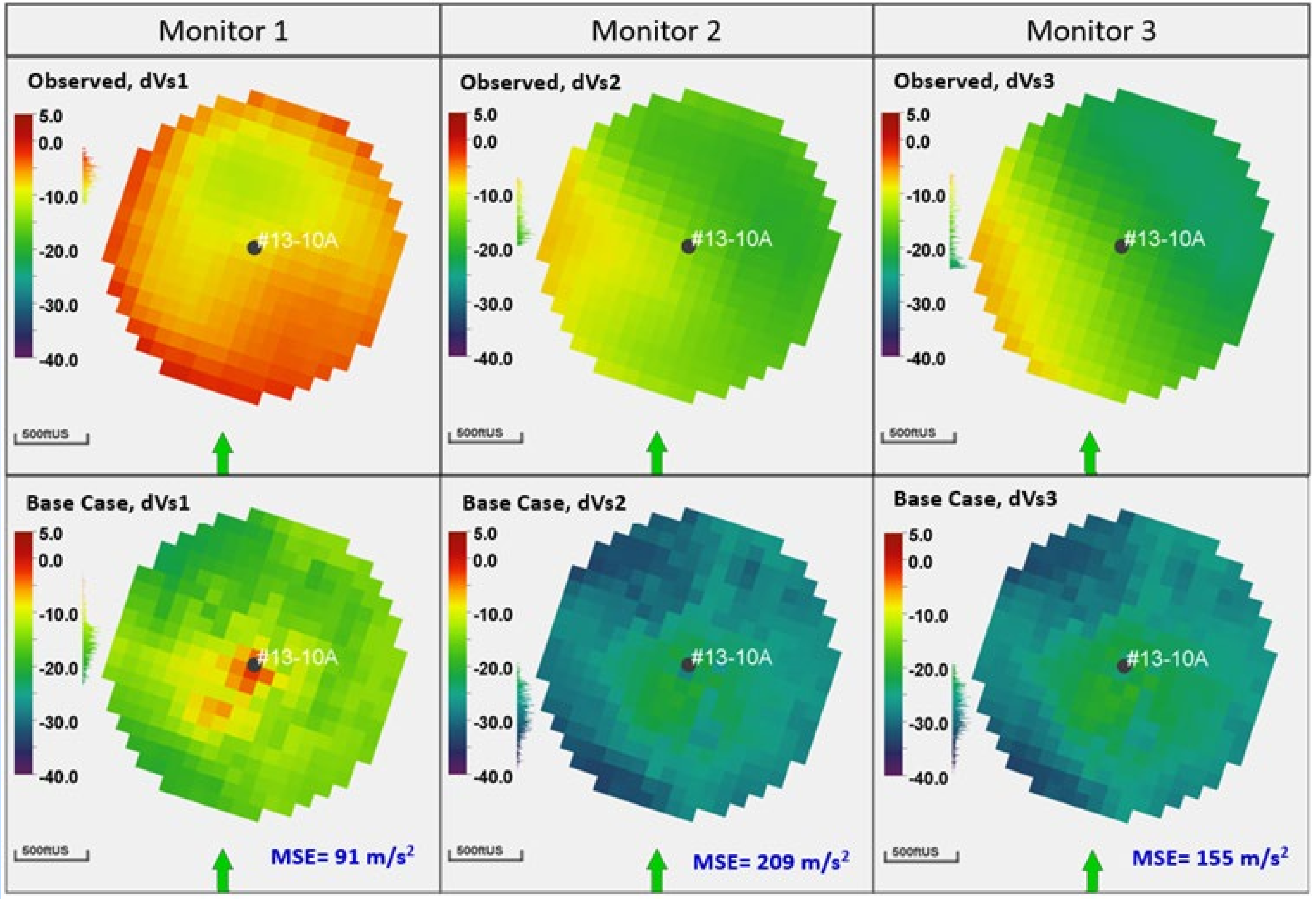

Time-Lapse Compressional Seismic Velocity Changes. Row 1 presents the observed dataset, and Row 2 represents the modeled compressional seismic velocity.

VSP- Geomechanical Calibration Task 7.4- dVs Calibration

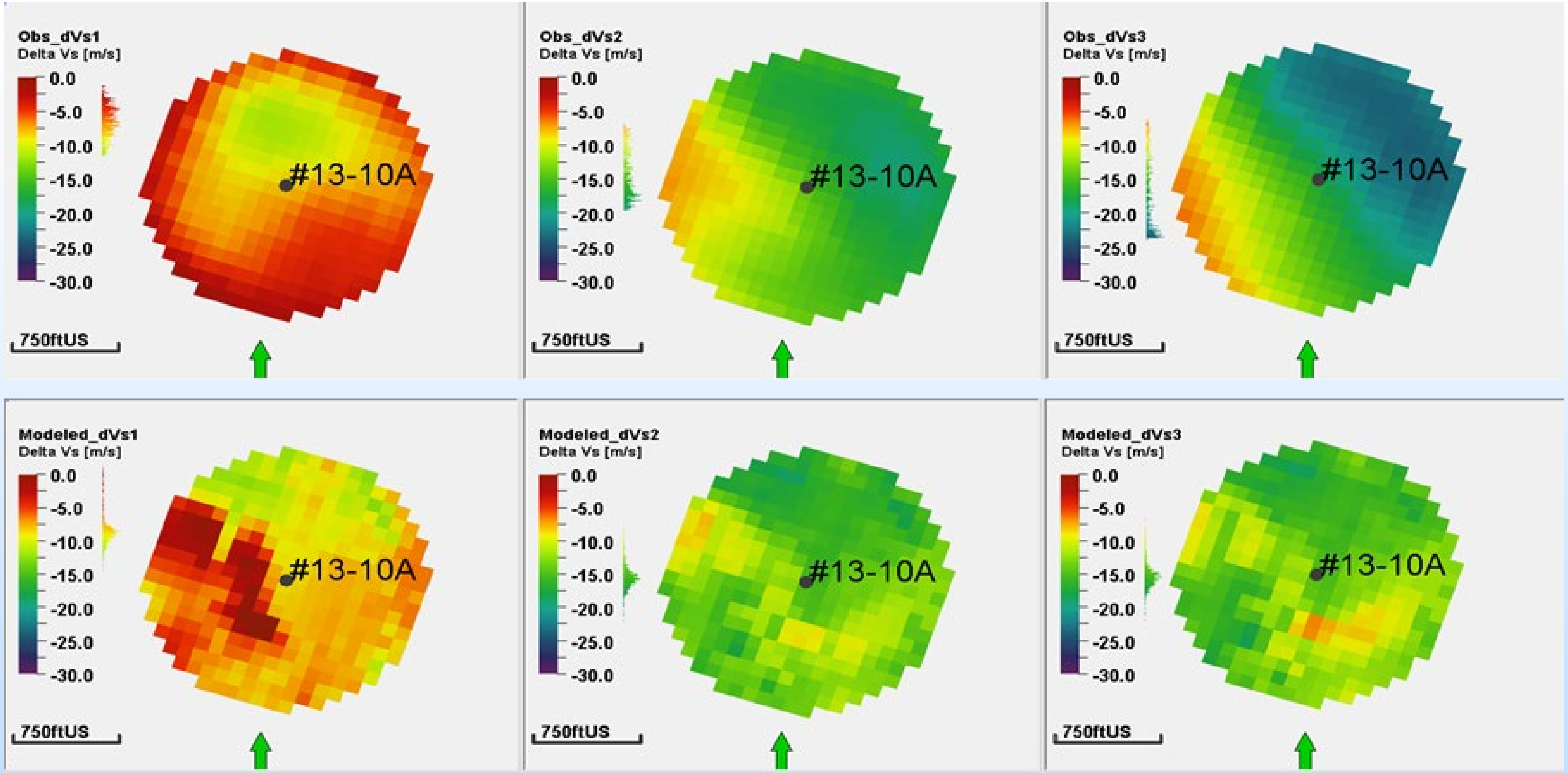

Time-Lapse Compressional Seismic Velocity Changes. Row 1 presents the observed dataset, and Row 2 represents the modeled compressional seismic velocity.